AN ABSTRACT OF THE THESIS OF

DAVID BRUCE ENFIELD for the MASTER OF SCIENCE
(Name of student) (Degree)

in OCEANOGRAPHY presented on MAY 1, 1970
(Major) (Date)

Title: A MESOSCALE STUDY OF COASTAL CURRENTS AND UPWELLING OFF PERU

Abstract approved: Redacted for Privacy
Dr. Robert L. Smith

Moored instrument records, drogue displacements, and hydrographic observations are used in describing the coastal currents and upwelling off Peru. The data were obtained over the continental shelf near 15° S. during a two week study in late March and early April of 1969.

First order statistics and graphical representations of current meter time series indicate that the longshore flow was poleward during most of the study period, interrupted by a three day 'event' of equatorward flow. The similarity of flow at all current meters indicates that the field of flow as quasi-barotropic. The depth, extent, and transport of poleward flow indicated by current meter time series and geostrophic sections were similar to those described in the literature for the Peru-Chile Undercurrent. The observations suggest that this flow moved further offshore as equatorward flow appeared over the shelf.

Power spectral analyses performed on current meter records

indicate the existence of semidiurnal tidal currents in the longshore direction. The magnitude of these currents is estimated at 10% to 15% of period mean speeds.

Ten meter drogue displacements are compared with 25 m recorded currents and with winds. The observations indicate that: the drogues were affected by both the 25 m flow and the wind; the depth of the wind drift layer was between 10 m and 25 m; the drogue displacements were in the sense expected from the Ekman model.

Vertical sections of sigma-t, oxygen, and nitrate indicate the existence of conditions consistent with upwelling. Surface maps of temperature, nitrate, and chlorophyll 'a' over the shelf are used to define the horizontal field of upwelling and its variations in time. The distributions suggest that upwelling existed throughout the period and underwent temporal and spatial modulations in intensity. The possibility of a causal mechanism between observed current and upwelling variations is examined.

Vertical salinity sections indicated the presence of a weak salinity minimum between the surface and 100 m. It is suggested that this minimum manifests the remnants of a tongue of Subantarctic Water embedded in a much larger mass of Equatorial Subsurface Water. The occurrence of the minimum only in conjunction with poleward flow suggests that the water was advected or mixed coastward somewhere north of the area studied, was entrained in the Peru-Chile Undercurrent, and was carried south again.

A Mesoscale Study of Coastal Currents and Upwelling off Peru

by

David Bruce Enfield

A THESIS

submitted to

Oregon State University

in partial fulfillment of
the requirements for the
degree of

Master of Science

June 1970

APPROVED

Redacted for Privacy

Associate Professor of Oceanography
in charge of major

Redacted for Privacy

Head of Department of Oceanography

Redacted for Privacy

Dean of Graduate Office

Date thesis is presented May 1, 1970

Typed by Opal Grossnicklaus for David Bruce Enfield

ACKNOWLEDGEMENTS

I would like to thank my major professor, Dr. Robert L. Smith, and Dr. June G. Pattullo for providing most of the professional guidance for this thesis. Many useful comments have also been contributed by Dr. Fred Ramsey, Dr. Lawrence Small, Dr. Douglas Caldwell, Dr. William Quinn, Mr. Dale Pillsbury and Mr. David Cutchin.

The formidable task of processing current meter and wind recorder data would not have been possible without the help of the staff of the Coastal Currents Project, including Miss Lillie Bogert, Miss Susan Van Dyke, Miss Marilynne Hakanson, Mr. Nathan Kieth, Mr. Mark Ebersole, and Mr. Joseph Bottero. Mr. William Gilbert and Mr. Ronald Hill drafted most of the figures.

I especially wish to thank Dr. Richard Dugdale of the University of Washington for inviting my participation in the PISCO cruise, and for his generous help in providing virtually all of the drogue and hydrographic data used in this thesis.

Ship support for the R/V THOMAS G THOMPSON and travel for the participants were provided by the National Science Foundation under NSF Grant GB 8648, as a part of the U. S. effort in the International Biological Program. Personnel and supplies for the cruise were provided under NSF Grant GA 1435. Data reduction expenses were paid for by the Office of Naval Research under ONR Contract

00014-67-A-0369-007. Current meters and thermographs were provided under NSF Grant 331; the wind recorder was provided under N ONR 1286(10). Travel for myself was provided under N ONR 1286.

I am indebted to my wife, Elena, for her patience and encouragement during the preparation of this thesis.

TABLE OF CONTENTS

LIST OF TABLES

LIST OF FIGURES

A MESOSCALE STUDY OF COASTAL CURRENTS AND UPWELLING OFF PERU

I. INTRODUCTION

Smith (1968), in an extensive review of the subject, defined upwelling as an ascending motion, of some minimum duration and extent, by which water from subsurface layers is brought to the surface layer and is removed from the area by horizontal flow.

The gross features of the physical process of upwelling have been defined by means of classical large scale, steady state considerations. If these efforts are to be improved upon, we must inquire further into the spatial and temporal variations of upwelling as well as the atmospheric factors, currents, and mixing associated with the process. This requires that investigative efforts be intensified and limited to smaller areas in order to achieve greater detail.

Smith, Mooers and Enfield (in press) have outlined the necessary elements for an effective mesoscale study of upwelling processes. To obtain adequate coverage for the characteristic lengths and periods involved in coastal upwelling, they recommend a study lasting several months over an area some 100 km long and 50 km wide, above the continental shelf and slope. The necessary physical data would include surface synoptic surveys of the area, direct measurements of vertical motion, shallow drogues, and time series of wind,

currents, and temperature, as well as standard hydrographic and STD casts. Although all of these are presently feasible, improvement of techniques and equipment is needed in most cases.

The 1969 expedition of the R/V THOMAS G. THOMPSON to Peru, called the PISCO cruise, was in part a first effort at such a mesoscale study, and in part a pilot project designed to determine the requirements for effective investigations in the future.

The study was conducted in a coastal zone between Pisco and San Juan, near 15^{o} S, where persistent upwelling had been indicated by previous investigations. In late March and early April, a wind recorder, current meters, and thermographs were moored over the continental shelf. During an intensive two week study, continuous wind, current, and temperature measurements were supplemented by bottle casts, shallow drogues, and surveys of surface properties.

The geographical location of the study and the spatial disposition of experimental activities are shown in Figure 1. Except for the hydrographic sections shown, almost all work was conducted over the continental shelf, within 30 km of the shore, in an area extending about 120 km along the coast.

An instrument array consisting of three separate taut-line moorings was installed on 28 and 29 March. On 9 April the two moorings shown in Figure 1 (CM-1 and CM-2) were recovered; the third mooring was lost. The array configuration for the two

recovered moorings is shown in Figure 2.

Seven drogues were set during the study, the first at a depth of 3.5 meters, and the succeeding six at ten meters. The two hydrographic sections shown in Figure 1 extended about 100 km offshore. Section I, off Punta San Juan, was taken on 31 March and 1 April; Section II, off Cabo Nazca, was taken on 3 and 4 April.

On a number of occasions the ship steamed on a zig-zag course over the shelf while an autoanalyzer measured near-surface temperature, nitrate, silicate, and chlorophyll 'a' at regular intervals. The data from these surveys were used to construct the surface maps of temperature, nitrate, and chlorophyll 'a' in Figure 12.

The basic objective of this thesis is to use the above data in describing the extent and variation of the coastal currents, their relation to the upwelling and winds, and their role in transporting water into the upwelling area.

In Chapter two, present knowledge pertinent to these topics is discussed. Chapter three describes the observational program of the PISCO study in greater detail. Data from the moored instruments and drogues are summarized and analyzed in Chapters four and five. In Chapter six the upwelling is described on the basis of hydrographic observations, and in Chapter seven the combined aspects of the upwelling and currents are discussed.

II. LITERATURE REVIEW

Roden (1962), in a study of the eastern equatorial Pacific, postulated a balance between the vertically integrated transport and the wind stress curl, enabling him to compute the mass transport streamlines from wind observations. The resulting total mass transport between 82° W. and the coast of Peru was southward, opposite to the prevailing winds and surface currents known to exist there (Gunther, 1936). Geostrophic speeds (Wooster and Gilmartin, 1961), geopotential topographies (Wyrtki, 1963) and maps of acceleration potential (White, 1969) have confirmed the tendency for such flow to occur. But in all of these studies the northward Peru Coastal Current (Gunther, 1936; Wyrtki, 1963) was found to split the southward flow into the nearshore Peru-Chile Undercurrent (Wooster and Gilmartin, 1961; Wyrtki, 1963; White, 1969) and the Peru Countercurrent which flows south offshore along the 80th meridian (Wyrtki, 1963; White, 1969).

In dynamic topographies of the sea surface, 100 decibar surface, and 200 db surface, Wyrtki (1963) showed the northward flow of the Peru Coastal Current between 78° W. and the coast of Peru. The flow became gradually confined to a narrower offshore band until it reached 15° S. Between 15° S. and 10° S. the flow turned shoreward at all levels. At the 100 db and 200 db levels the flow

returned to the south with the Peru-Chile Undercurrent. Wooster and Gilmartin (1961) and Wyrtki (1963) showed that very little remained of the northward flow north of 10° S.; at 5°S. (Punta Aguja, Peru) the Peru Countercurrent and Peru-Chile Undercurrent formed a single southward flow.

Wooster and Gilmartin (1961) confirmed the existence of the poleward Peru-Chile Undercurrent by drogue measurements. Wyrtki (1963) found the flow to be strongest at depths of 100 m and 200 m, and estimated the mass transport at 0.5 to 1.0 million cubic meters per second. Wyrtki (1966) added that north of 15° S. the flow is found immediately below a shallow layer of equatorward wind drift. In their geostrophic sections, Wooster and Gilmartin (1961) showed that the volume transport decreased considerably as the undercurrent progressed southeastward along the coast, and the speeds decreased from 20 centimeters per second at 5° S. to 2 cm/sec at 15° S. Hart and Currie (1960) noted similar decreases in the flow of the subsurface countercurrent off West Africa. They suggested that the depletion occurred as the current supplied the water for upwelling near the coast. Wyrtki (1963) observed that the Peru-Chile Undercurrent supplied the upwelling off Peru with water from the north.

Near 15° S. off Peru, the water masses found in the upper 500 m are Equatorial Subsurface Water, Subantarctic Water, and Subtropical Surface Water.

Wyrtki (1963) defined Equatorial Subsurface Water as water whose temperatures and salinities occupy a regression line between 17°C., 35.2‰ and 7°C., 34.6‰, and which is found along the equatorial Pacific in a depth range between 50 m and 500 m. He speculated that the eastward flow of the Equatorial Undercurrent was responsible for the accumulation of this water in the eastern tropical Pacific, off Peru and Ecuador. The distribution and characteristics of Equatorial Subsurface Water are essentially those of Equatorial Pacific Water as defined by Sverdrup, Johnson, and Fleming (1942).

Salinity sections along the South American coast were discussed by Gunther (1936) and Wooster and Gilmartin (1961). These sections show that south of 15° S. the Equatorial Subsurface Water is found as a tongue of relatively high salinity extending south, with the fresher Subantarctic Water and Antarctic Intermediate Water above and below. The Subantarctic Water is in turn manifested as a tongue of less saline water extending north, overlain by the salty Subtropical Surface Water between 23° S. and 15° S. Wyrtki (1963) pointed out that the Peru Coastal Current carries the Subantarctic Water as far north as 15° S. where it is present only as a weak salinity minimum above 100 m and in the lower portion of the pycnocline, overlying the salinity maximum of the Equatorial Subsurface Water.

Wyrtki (1963) characterized Subtropical Surface Water off the Peru coast by salinities in excess of 35.0‰ and temperatures between

17° and 20° C. It overlies most of the region as a shallow surface layer and is separated from the coast south of 15° S. by a narrow band of upwelled, less saline Subantarctic Water; north of 15° S. it is displaced as much as 500 km offshore by upwelled Equatorial Subsurface Water of lower temperature and slightly lower salinity. Wyrtki's (1963) transport computations implied that the upwelling south of 15° S. is supplied by Subantarctic Water flowing north with the Peru Coastal Current, and north of 15° S. by Equatorial Subsurface Water flowing south with the Peru-Chile Undercurrent.

Wooster and Reid (1963) pointed out that cross stream density profiles in coastal upwelling zones frequently show a nearshore weakening of the vertical density gradient at depths of 100 m to 200 m. They observed that poleward undercurrents and the boundary processes of upwelling and enhanced vertical mixing are associated with the shoreward rise and fall of isopycnals above and below the weak density gradient. Yoshida and Tsuchiya (1957) discussed the same feature of cross stream profiles. They showed, on theoretical grounds, that a dynamic balance takes place between the horizontally convergent flow of a coastal undercurrent and the rise of water to the surface in upwelling. They also stipulated that the weak density gradient feature may be used as an indicator of upwelling, but cautioned that poleward flow would not normally result in the lower layer during the transient stages of upwelling, rather, only after

an established state had been reached.

Gunther (1936) examined the depth of water affected by upwelling at 12 latitudes along the coast of Peru, and arrived at an average estimate of 130 m. Wyrtki's (1963) study of the vertical and horizontal field of motion indicated that the upwelling along the coast was limited to depths of less than 100 m. He added, however, that ascending motion at greater depths and further offshore was of the same magnitude as the coastal upwelling and was presumably important in the upwelling process.

Several workers have described a decrease in the mixed layer depth going from south to north along the Peru coast (Mejía and Poma, 1966; Guillén and Flores, 1967; Miñano, 1968). Miñano (1968) found average depths of 86 m, 65 m, and 53 m in the southern, central, and northern regions of the Peru coast, respectively.

Hart and Currie (1960) cautioned that isotherms which ascend toward the coast but exhibit a strong vertical gradient should be considered a relic of previous upwelling, rather than evidence of active upwelling at the time of observation. Schweigger (1958), in a study of upwelling off Peru, pointed out that the vertical mixing produced by the upwelling does not allow the formation of a thermocline, or if so, only an insignificant one.

Wooster and Reid (1963) made the observation that intense coastal upwelling was indicated when nearshore surface waters were

significantly undersaturated in dissolved oxygen. Posner (1957) reported the occurrence of such undersaturation associated with upwelling along the Peru coast.

Schweigger (1958) distinguished five regions of upwelling along the coast of Peru. He characterized the area between 14° S and 16.5° S as having the coldest temperatures and consequently the strongest upwelling. He described the region as one where aspiration contributes significantly to the upwelling process, that is, enhanced upwelling results due to increased horizontal divergence as the Peru Coastal Current flows past the coastal prominence at 14° S.

III. OBSERVATIONAL PROGRAM

The physical observations made during the PISCO study may be subdivided into three operational phases:

(i) time series measurements of currents, wind, and temperatures by moored instruments;

(ii) shallow drogue experiments;

(iii) hydrographic sampling program, consisting of bottle and STD casts, and surveys of surface properties.

Self-contained recording instruments were moored off the coast on 28 and 29 March to measure currents, temperature, and wind. The positions and depths of the various array elements are shown in Figures 1 and 2. Current meters were placed at 25 m and 50 m at the inshore mooring (CM-1), and at 25 m, 50 m, and 135 m at the offshore mooring (CM-2).

Current meters were not placed at depths shallower than 25 m, in order to avoid wind effects, mooring motions, and surface wave contamination of the data. By placing instruments at depths of 25 and 50 m, it was hoped to measure the currents across the pycnocline and determine the vertical current shears there. Previous investigations cited in the LITERATURE REVIEW have pointed to the probable existence of a poleward undercurrent adjacent to and over the continental shelf, at depths of 100 to 200 m. To measure the

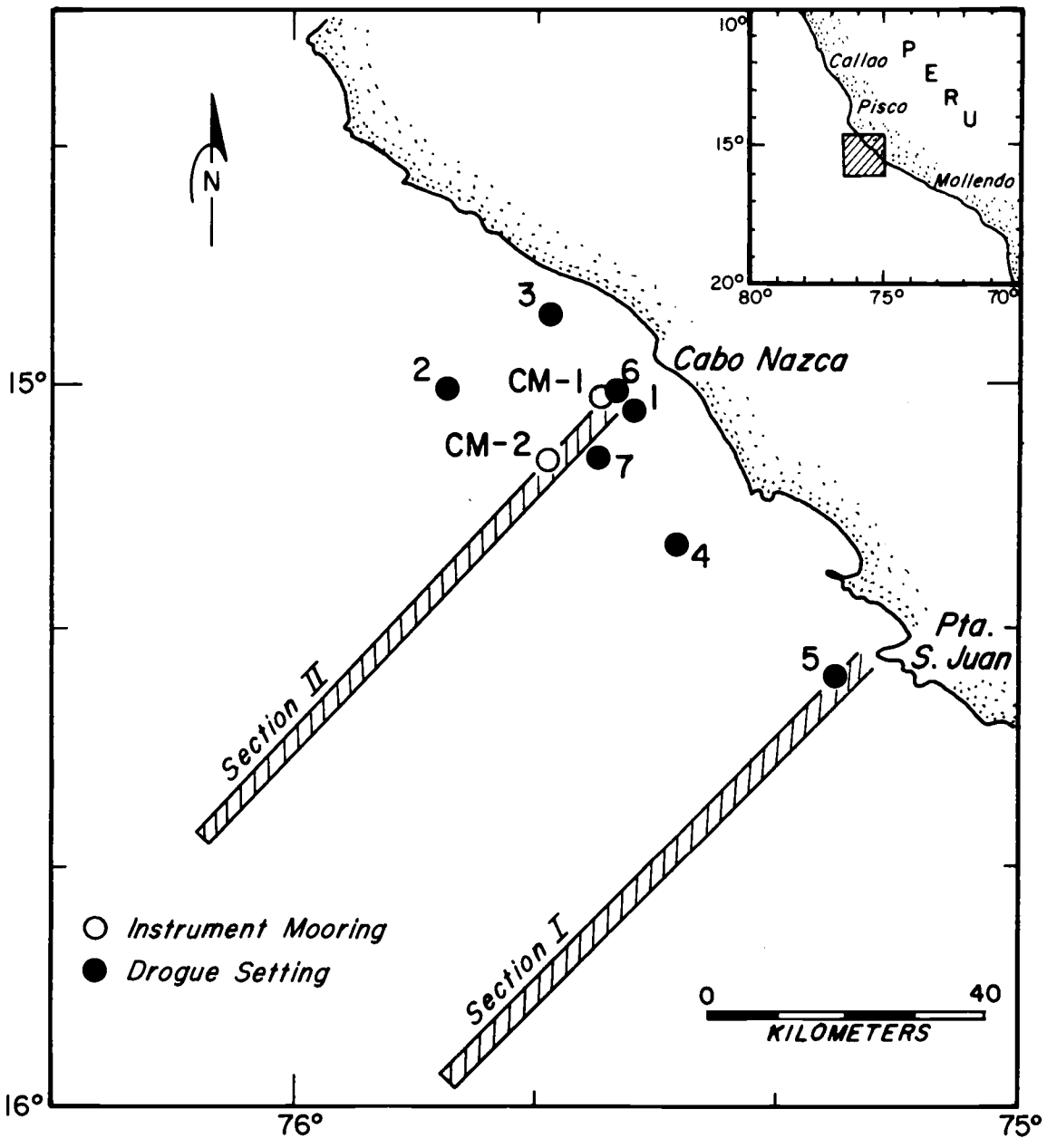

Figure 1. Location of the PISCO study and positions of moored instruments, drogues, and hydrographic sections.

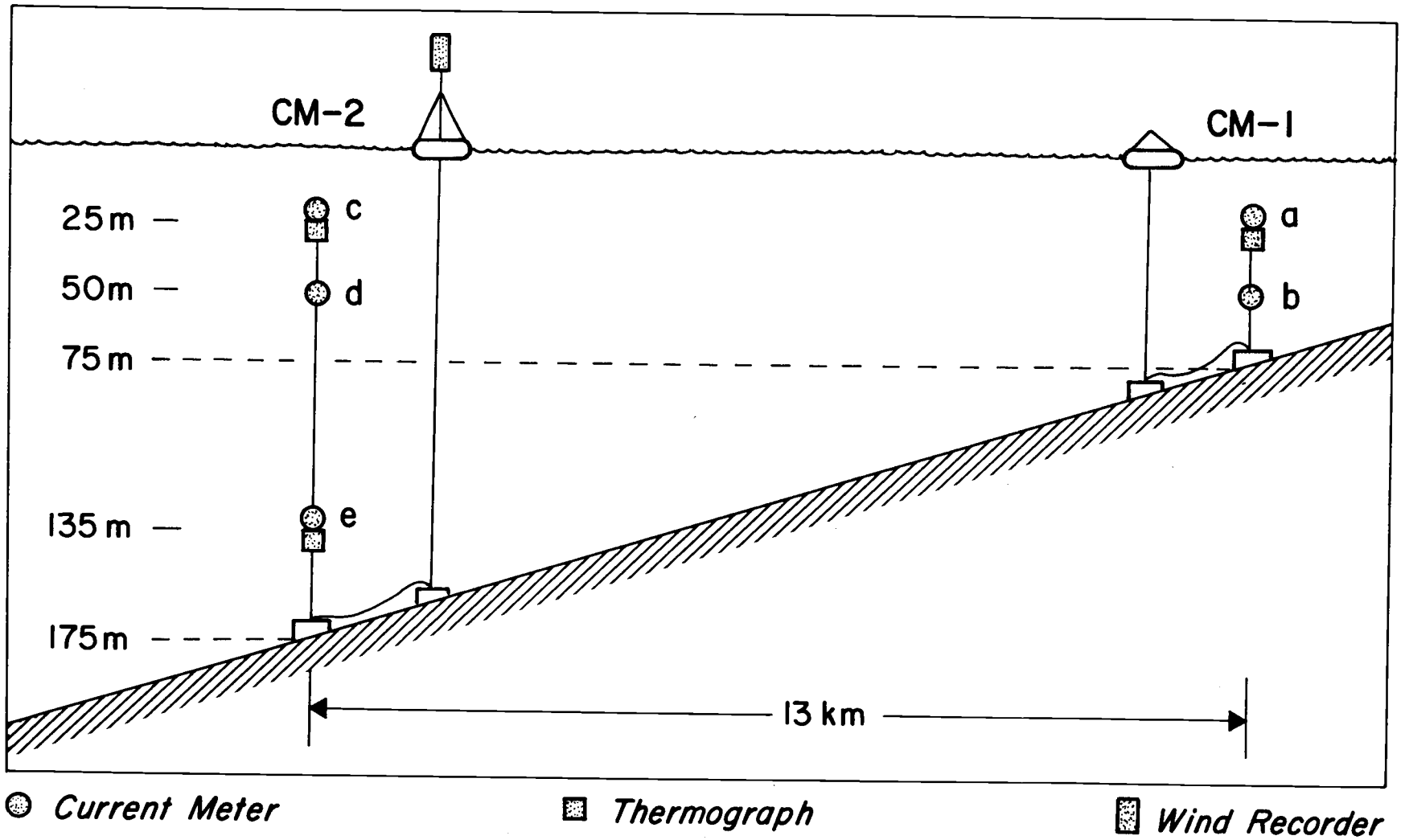

Figure 2. Configuration of the moored instrument array.

Peru-Chile Undercurrent, a current meter was placed at a depth of 135 m, offshore (CM-2).

In addition to the current meters, thermographs were placed at 25 m, inshore and offshore, and at 135 m offshore. A wind recorder was placed at the offshore mooring (CM-2) to determine possible correlations between the behavior of the wind and that of the currents and upwelling. This instrument was placed at the offshore mooring (CM-2) to minimize the effects of land-induced diurnal variations.

The taut-line mooring technique used (Figure 2) has been discussed by Pillsbury, Smith and Tipper (1969). To minimize mooring motions, only subsurface floats were used to provide positive buoyancy. At each mooring, an auxiliary anchor was connected to the main anchor by means of a ground line several hundred meters in length. The position of the mooring was then marked by a surface toroid buoy tethered to the auxiliary anchor. The wind recorder was mounted on the surface toroid offshore and measured wind speed and direction at a height of about two meters above the water.

Current velocity was measured by Braincon Histogram Current Meters. The current meters sense speed by means of a Savonius rotor, the output of which is recorded on film in analog format. During each 20 minute recording period, between film advances, an arc is registered on the film, the length of which is proportional

to the total revolutions of the rotor during the recording period. The direction sensing device consists of a luminous compass dot whose orientation with respect to a casing mark can be determined from the film. If the orientation of the instrument changes during a 20 minute sampling interval, which is invariably the case, the compass dot also produces an arc. The length of the speed arc is assumed to be proportional to the average current speed during the sampling interval; the direction mode, indicated by the brightest part of the direction arc, is taken to be the mean direction. An implicit assumption in the use of such data is that the mean speed and direction so determined are representative of the vector mean velocity during the sampling interval. Such an assumption is valid only to the extent that relatively little directional variation occurs during the interval. The vector mean as estimated by this method is in general greater than the true value, although large discrepancies usually only occur at low current speeds, when the directional response of the instrument is poor. An indication of instrument tilt is also produced on the film, from which a correction to the measured current speed can be applied.

The operational principle of the Braincon Histogram Wind Recorder, used in this study, is similar in most respects to that of the current meters, as outlined above. The instrument is provided with a tilt indicator of the same design as that used in the current meters.

Unlike the current meters, however, the wind recorder undergoes many different tilting motions during a sampling interval, so that the indicator does not remain in any one place long enough to expose the film. To assess the possible error introduced by the tilt, static wind tunnel tests were conducted with the rotor tilted from its normal position by angles of up to 25°. At 25° tilt the speeds were consistently less, but only by barely observable amounts, indicating that instrument tilt in itself is not a serious source of error. Since calibration was performed in a wind tunnel, buoy motion and atmospheric turbulence have not been accounted for and presumably represent sources of error.

Water temperature was measured by Braincon Recording Thermographs, using a sampling interval of ten minutes. The temperature during each sampling interval was recorded on photographic film by means of a mercury thermometer placed between the film and a small light source. The extent to which the mercury column prevented exposure of the film was a measure of the temperature.

Specifications of instrument performance characteristics and calibration have been presented and discussed by Collins (1968) for the current meters and thermographs. Further discussion of the wind instrument is to be included in a future data report, now in preparation.

A graphical summary of the data retrieved from the moored

instruments is given in Figure 3. The full recording period, from the installation on 28 March to the recovery on 9 April, was about 12 days.[1] The two thermographs at the offshore mooring (CM-2), shown in Figure 2, failed completely, and are not included in the retrieval summary of Figure 3. The speed sensor of the current meter at 50 m, inshore (CM-1), failed on 7 April. The current meter at 135 m, offshore, failed to record speed and direction after 5 April. About six hours of data at the beginning of the current record for 50 m, offshore, was not obtained due poor readability of the film. The remaining instruments functioned satisfactorily and yielded data for the entire period.

To avoid undesirable shallow water effects, current meters were not placed at depths of less than 25 m. To determine the near-surface flow, shallow drogues were therefore set during the study. Each drogue consisted of a current cross suspended from a surface float, so as to catch the flow at a prescribed depth.

At the time of every drogue launch, radar fixes were taken on the nearest recognizable points of land, and a wind reading was taken from the ship's aerovane. At recovery, radar fixes were again taken.

The launch positions, numbered in chronological sequence, are

---

[1] For consistency, all date symbols appearing in the figures refer to 00 hours, GMT, on the indicated date.

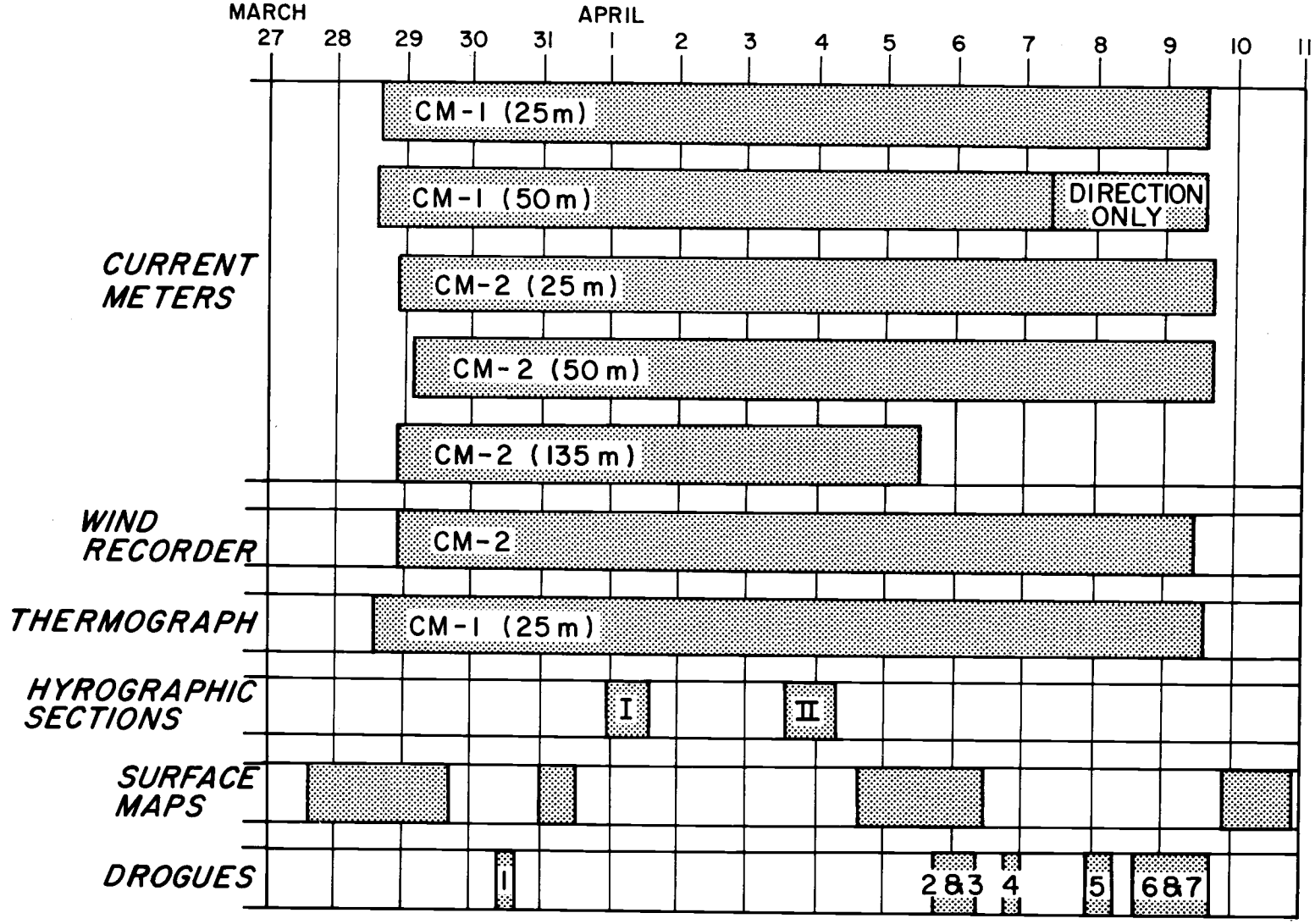

Figure 3. Summary of data retrieved. Vertical lines refer to 00 hours (GMT) on the indicated date.

shown in Figure 1. The times (GMT) during which the drogues were in the water are shown in Figure 3. All drogues except for the fifth were launched within 20 kilometers of the instrument array. Only drogue seven was left in the water for more than one semidiurnal tidal period.

Supplementary hydrographic operations were of two kinds: standard bottle and STD casts, and surveys of surface properties. Bottle casts were taken along two offshore lines to almost 100 km offshore, as shown in Figure 1. The first hydrographic line, Section I, was taken off Punta San Juan on 31 March and 1 April. The second line, Section II, was taken off Cabo Nazca on 3 and 4 April. The times (GMT) in relation to other data are shown in Figure 3. A number of shallow stations and short sections were taken over the continental shelf.

On a number of occasions, an underway Data Acquisition System was used to make maps of temperature, nitrate, silicate, and chlorophyll 'a'. While the ship steamed along a zig-zag course over the continental shelf, water samples were continuously drawn from a depth of 3 m. These samples were analyzed for the given properties at four-minute intervals by an autoanalyzer and the measurements were logged on paper tape. The tape records from the DAS were processed on board the R/V THOMPSON by an IBM 1130 computer and CalComp plotter to give contoured maps of the

properties. The interested reader may refer to Armstrong, Stearns and Strickland (1967) for a discussion of the use of autoanalyzer techniques in the underway recording of surface properties.

IV. TIME SERIES FROM MOORED INSTRUMENTS

The data retrieval summary for the moored instruments and drogues has been included in Figure 3. Five current meters, a wind recorder and a thermograph, located as shown in Figures 1 and 2, yielded time series varying from eight to 12 days in length.

In processing current meter and wind recorder data, the films were first scanned, the raw data were punched on cards, and several error detection programs were applied to them. The corrected data were processed by a program which resolved speeds and directions into velocity components parallel and perpendicular to the coast (longshore velocity positive to the northwest; onshore velocity positive toward the coast). The details of the data processing and the programs used are discussed by Mooers (et al., 1968).

In the second phase of the processing, first order statistics, including means, standard deviations, maxima, minima, and primary and secondary modes were obtained, and are summarized in Table 1. For current measurments, relative frequencies were computed for intervals of 1 cm/sec in speed, 5 cm/sec in the component velocities, and ten degrees in direction. For winds, intervals of 0.2 knots in speed, 1 knot in the component velocities, and ten degrees in direction were used. Since the speed and direction averages are scalar means, they cannot in general be combined in polar form to produce a vector

Table 1. Statistics from moored instruments.

Mooring location	Depth (m)	Number of observations	Variable	Mean	Standard deviation	Maximum	Minimum	Principal Mode	Principal r.f. (%)	Secondary Mode	Secondary r.f. (%)
Current statistics											
CM-1	25	859	Speed, cm/sec	17.6	6.7	39	6	12	18.5	--	--
			Onshore, cm/sec	3.2	6.7	20	-15	0	27.9	--	--
			Longshore, cm/sec	-8.6	15.0	30	-40	-10	23.1	10	9.2
			Direction, °True	169	138	--	--	120	12.8	330	4.1
	50	702	Speed, cm/sec	22.5	10.7	48	9	12	14.0	35	4.4
			Onshore, cm/sec	0.7	6.4	15	-15	0	31.3	--	--
			Longshore, cm/sec	-15.4	18.5	20	-50	-10	16.7	-35	14.1
			Direction, °True	162	83	--	--	130	27.1	335	3.4
CM-2	25	845	Speed, cm/sec	23.7	10.6	53	9	12	7.2	31	3.6
			Onshore, cm/sec	4.2	6.8	25	-30	5	28.2	--	--
			Longshore, cm/sec	-17.9	16.6	25	-55	-10	14.9	-30	13.3
			Direction, °True	148	73	--	--	120	17.6	320	3.3
	50	831	Speed, cm/sec	22.5	8.9	48	6	28	5.8	16	4.3
			Onshore, cm/sec	4.6	8.5	30	-15	0	22.0	--	--
			Longshore, cm/sec	-15.2	16.1	35	-50	-25	21.7	--	--
			Direction, °True	146	77	--	--	130	17.0	330	3.0
	135	542	Speed, cm/sec	10.4	5.8	25	2	7	10.5	16	7.2
			Onshore, cm/sec	-0.7	3.4	20	-10	0	53.9	--	--
			Longshore, cm/sec	-6.6	9.2	10	-25	-15	22.7	5	22.7
			Direction, °True	179	72	--	--	130	20.9	250	6.1
Wind statistics											
CM-2		827	Speed, knots	8.9	3.0	14	1	10.5	10.7	--	--
			Onshore, knots	4.2	2.3	8	-1	5.0	20.3	7.0	12.6
			Longshore, knots	7.5	2.9	13	0	8.5	23.0	5.0	13.4
			Direction, °True	163	16	190	100	170	22.2	--	--
Temperature statistics											
CM-1	25	1718	Temperature °C	16.2	0.3						

mean velocity. Such a vector mean will result, however, when the averaged component velocities are combined.

One of the salient features of the data, as summarized in Table 1, is the occurrence of two, nearly opposite direction modes at all current meters. The 20-minute direction measurements were most frequently toward 120° or 130°, i.e., longshore to the southeast, and slightly onshore. The second most frequent direction (except for the deepest current meter) was toward 320° or 335°, i.e., longshore to the northwest, and also slightly onshore. The current meter at 135 m, offshore, showed a tendency for offshore flow in the secondary mode. This instrument functioned only for eight days, therefore caution must be exercised in comparing its statistics with those of the other instruments.

Measured speeds were greater in the primary, or southeastward mode, than in the secondary, or northwestward mode. Speed measurements tended to be greater in the longshore direction than in the onshore sense.

Wind speed measurements varied from a near calm to a maximum of 14 knots, with a mean of 8.9 knots and a standard deviation of 3.0 knots. Measured wind directions were consistently from the southeast, being from 163° on the average, with extremes of 100° and 190°.

As pointed out by Collins (1968), such statistical summaries

give no information as to the time scale on which the indicated variations take place. For example, the bimodal directions exhibited by the current statistics could be interpreted on the one hand as having been produced by successive mean longshore flows in opposite directions, or alternatively, as the result of oscillatory longshore tidal currents.

To obtain an alternative, graphical representation of the data, cumulative sums of onshore and longshore velocity components were computed and plotted against each other in what is termed a progressive diagram, or PVD. The PVD's for current and wind measurements are shown in Figures 4 and 5, respectively. The use of such diagrams has become widespread, since they afford a convenient graphical representation of a vector time series. A straight line drawn between any two points of a PVD represents the vector mean velocity during the corresponding interval of time. A PVD is constructed in the Eulerian sense, i.e., from a series of measurements at a fixed point, and therefore does not in general represent the trajectory (Lagrangian sense) of a fluid parcel. For further discussion, see Collins (1968).

Figure 4 shows the progressive vector diagrams for the five current meters, corresponding to the lettered array positions in the schematic of Figure 2. The distance between any two points on the PVD's may be measured against the horizontal scale, given in

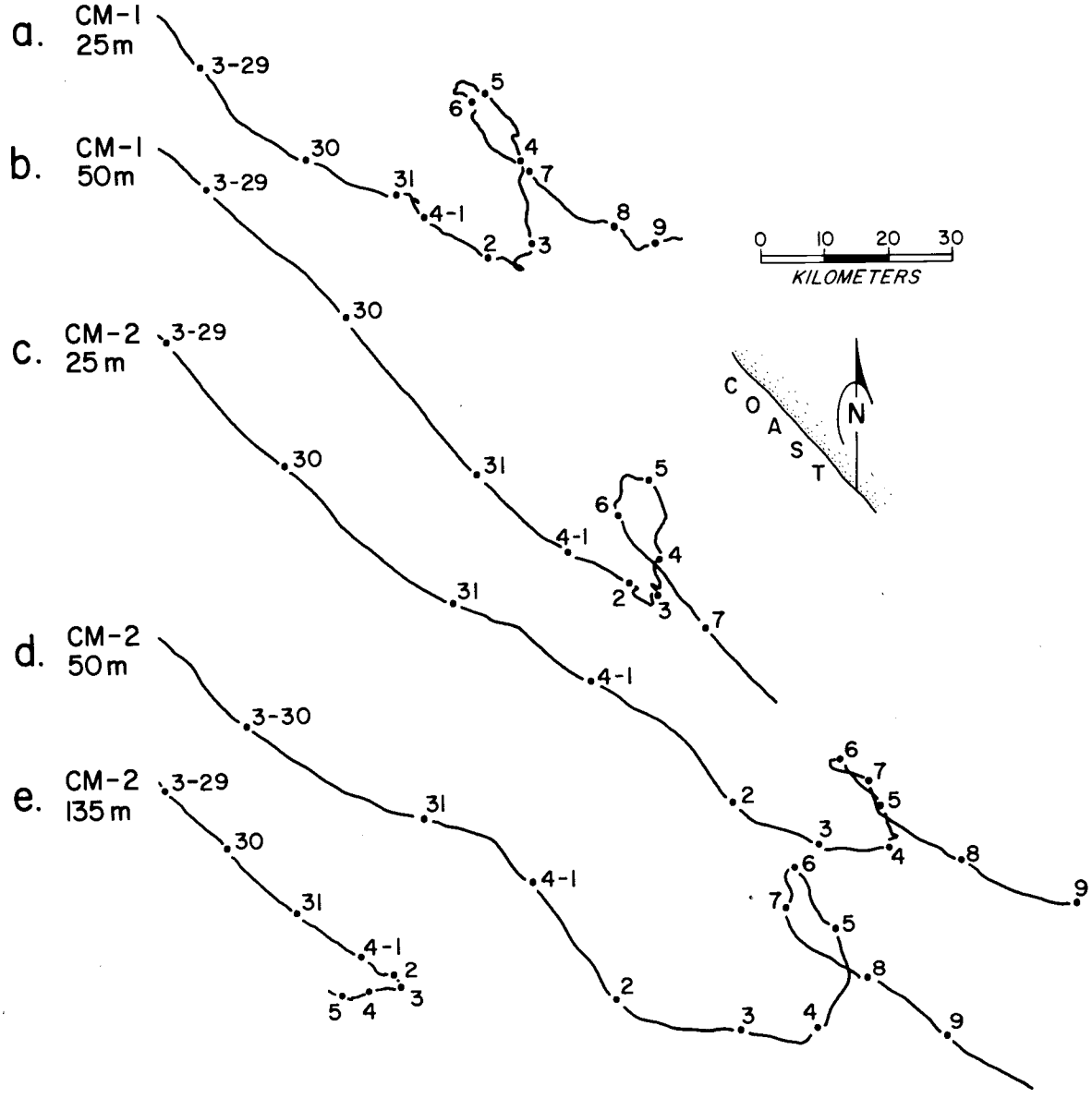

Figure 4. Progressive vector diagrams of the recorded currents. Symbols refer to 00 hours (GMT) on the indicated date.

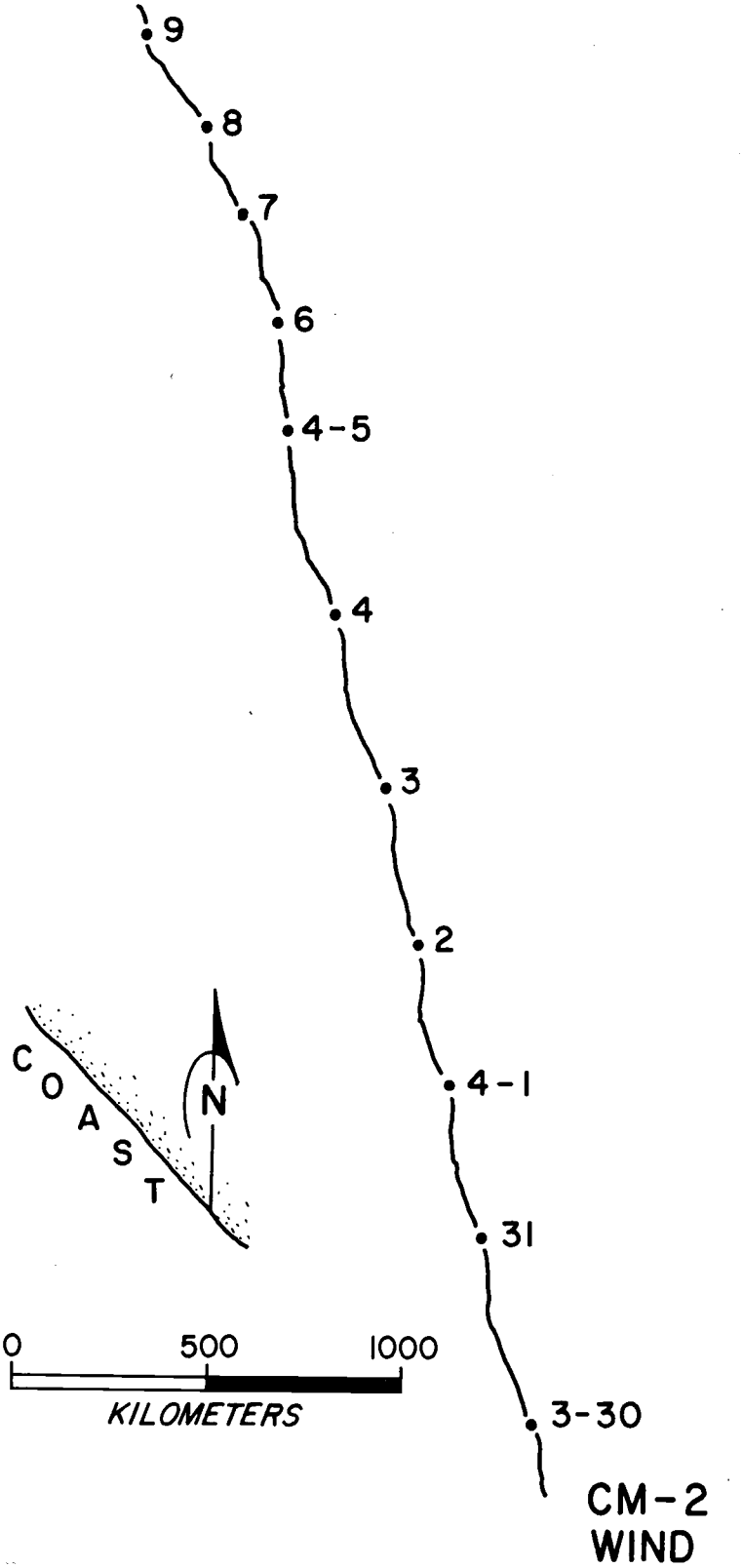

Figure 5. Progressive vector diagram of the recorded wind. Symbols refer to 00 hours (GMT) on the indicated date.

kilometers, and divided by the corresponding time interval to obtain the speed of the vector mean current.

The PVD's indicate that the flows at all current meters were similar in the sense that all exhibited predominantly southeastward flow. In addition, all but the deepest current meter underwent a northward 'event' during the period of 2 April to 5 April, inclusive. During this time, the flow at 135 m was mostly offshore, just prior to the failure of that instrument. It is clear that the bimodal directions of Table 1 are in fact related to mean flows, and not to tidal or other relatively short-period variations. The current field was essentially quasi-barotropic, as evidenced by the uniform measurement patterns.

Figure 5 shows the PVD for the recorded winds. There is considerable constancy in direction for time intervals exceeding a day. Most of the variance exhibited by the wind statistics (Table 1) is evidently associated with a marked diurnal, or seabreeze oscillation, as can be seen from the undulatory character of the PVD. The spacing of successive midnights (GMT) indicates a decreasing trend in the daily mean speeds.

Daily means were computed for the onshore and longshore components of current and wind velocities, with each mean centered at 1200 hours, GMT. The time series of daily mean longshore velocities are shown in Figure 6.

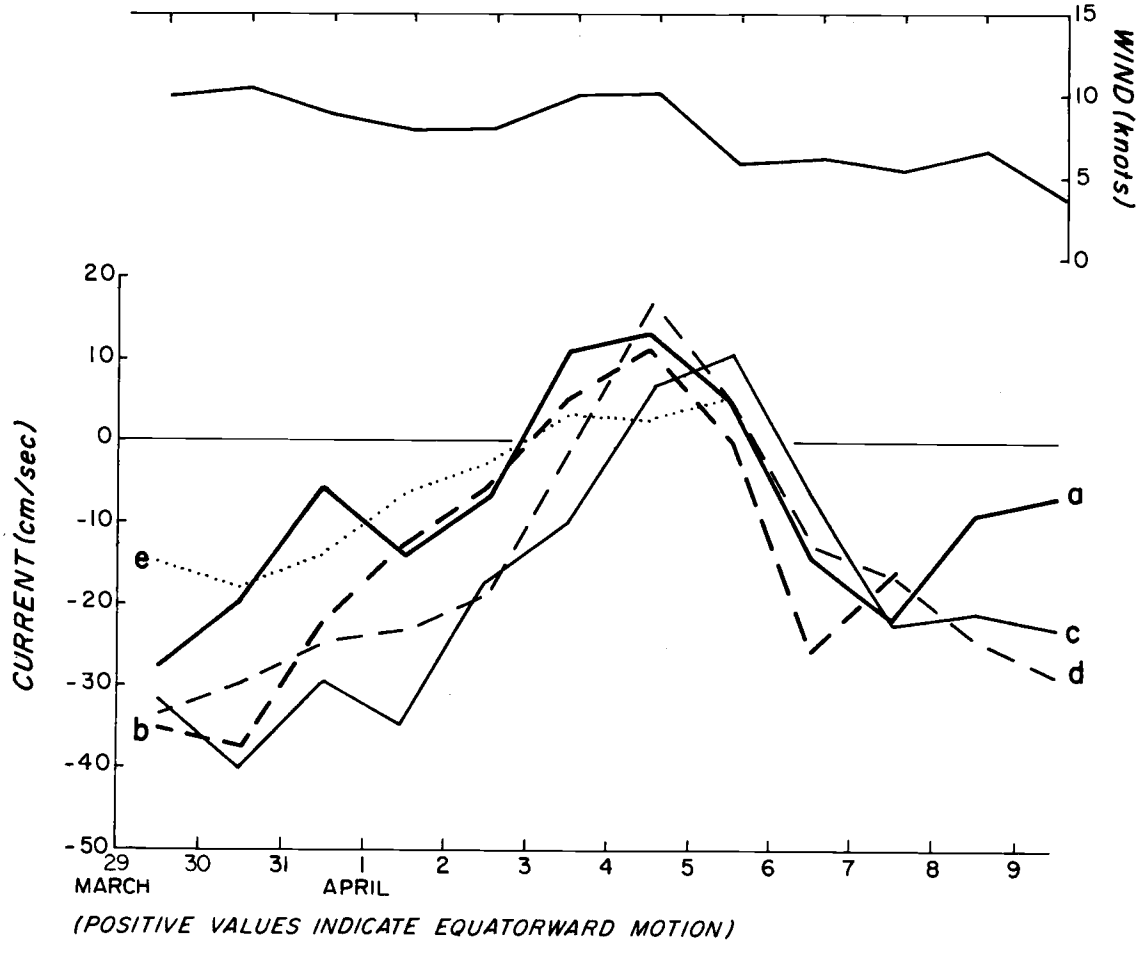

Figure 6. Time series of daily mean currents and wind. Time marks refer to 00 hours (GMT) on the indicated date.

a. Current at 25 m inshore (CM-1).
b. Current at 50 m inshore (CM-1).
c. Current at 25 m offshore (CM-2).
d. Current at 50 m offshore (CM-2).
e. Current at 135 m offshore (CM-2).

While the similarity between the currents at different locations is again evident, it is clear from Figure 6 that the 'event' was not a sudden occurrence, but the climax of a gradual decrease and reversal of the poleward (southeastward) flow. At 25 m, equatorward flow first appeared at the inshore station more than a day prior to its appearance offshore. A similar lag (1/2 day) was observed at 50 m.

The daily mean longshore component of the wind showed a decreasing trend during the period, from about ten knots to about five knots. Superimposed on the trend is a modulation with a periodicity of about a week. The plot (Figure 6) is an index of daily mean wind speeds as well, since the direction was consistently from the southeast.

The single thermograph which yielded data was located at 25 m depth inshore (CM-1), and the data record retrieved was complete (Figure 3). The recorded temperatures were essentially constant for the entire period, with a mean of 16.2° C. and a standard deviation of 0.3° C. (see Table 1).

V. ANALYSIS OF CURRENTS

The discussion of the currents may be conveniently divided into two phases, according to the character of the data which are examined: (i) a current meter analysis, and (ii) a drogue analysis.

The first phase of analysis treats the time series from the moored current meters, complemented by geostrophic sections. The time series from the instrument array define a field of currents with time variations in the Eulerian sense. The records may therefore be subjected to a variational, or time series analysis, and they may also be examined in a spatial sense, with the aid of the computed fields of geostrophic currents. The time and space domains which can be analyzed are essentailly limited by the temporal and spatial resolution and extent of the data.

The drogue observations, unlike the current meter records, were taken in the Lagrangian sense, and were limited to the surface boundary layer. The drogues do not define a field, and they define a series only by the sequential manner in which they were launched. But since the drogues were presumably affected by both the wind and by the overall field of water flow, they may be analyzed in conjunction with wind recorder and current meter measurements.

Current Meter Analysis

The current meter observations were taken at equally spaced 20-minute sampling intervals for periods of eight to 12 days. It is possible to statistically analyze such records for periodic phenomena of frequencies between about one cycle per hour and one cycle per day. This frequency range includes both the semidiurnal (2.0 cpd) and diurnal (1.0 cpd) tides, but does not include inertial oscillations at 15^{o} of latitude (0.5 cpd). To determine the extent of the tidal components, an autospectral analysis was performed on the current records.

Since the lowest frequency of interest within the given range was about 1 cpd, it was decided to compute autocorrelations for lags of up to 36 hours. This provided ten degrees of freedom for the shortest record (seven to eight days) and 15 degrees of freedom for the longest record (12 days). The frequency bandwidth for a maximum lag of 36 hours is about 0.7 cpd. This is just barely sufficient to resolve the diurnal frequency from either the semidiurnal or low frequencies. But spectral estimates at the diurnal frequency are presumably subject to some contamination from any inertial energy which may be present. No prewhitening or prefiltering of the data was performed. Aliasing problems do not arise for such current records, since each measured value is an average over the previous

20-minute sampling interval.

Autospectral analyses were performed on the onshore and longshore components of each current record. None of the onshore components showed significant spectral peaks at either tidal frequency. All longshore components exhibited semidiurnal spectral peaks which were significant at the 90% confidence level; diurnal spectral peaks were not found. Table 3 presents the results of the autospectral analyses for the semidiurnal longshore components. The estimated amplitudes of the semidiurnal longshore currents were about 10% to 15% of the period mean (measured) speeds.

The cotidal charts of Bogdanov (1961) for the South Pacific show that the semidiurnal tides in the geographical area of the PISCO study are essentially progressive waves propagating southward along the South American coast. Standard tables of predicted tide levels show that tidal amplitudes are of the order of one to two feet, with relatively little diurnal inequality. The results of the spectral analysis are therefore consistent with these sources.

Inertial oscillations, if they are significant in comparison with mean flows, should be manifested as counterclockwise loops on a progressive vector diagram (in the southern hemisphere). The PVD's of Figure 4 exhibit fairly uniform patterns except for the counterclockwise loop associated with the 'event' of 2 to 5 April. Careful examination of the PVD's reveals that the period for which the

Table 2. Spectral energies and estimated amplitudes of semi-diurnal currents.

Current meter mooring	Depth (m)	Record length (days)	Semi-diurnal spectral energy (cm^2/sec^2)	Estimated semi-diurnal current amplitude (cm/sec)	Period mean current speed (cm/sec)
inshore	25	12	8.0	2.8	18
"	50	10	8.7	3.0	22
offshore	25	12	7.5	2.7	24
"	50	12	5.9	2.2	23
"	135	8	1.9	1.4	10

current direction was significantly different from the mean southeastward trend was about three days, as contrasted to the inertial period of two days at 15° latitude. The loop in the PVD's can be seen as a quasi-sinusoidal oscillation in the plots of daily mean longshore flows (Figure 6). When considered in this way, the 'event' seen in the PVD's appears to have a total duration of some five days to a week. It does not seem likely therefore that significant inertial motion occurred during the study.

The data records are too short to determine if the observed oscillation just described is in fact an event-like phenomenon, or alternatively, one in a series of such oscillations with periods of about a week. But it is possible, by combining geostrophic computations with current observations, to construct two current sections extending from the coast to about 100 km offshore. The first section corresponds to the hydrographic line (Section I) shown in Figure 1, off Punta San Juan, which was taken on 31 March. The second section corresponds to the hydrographic line (Section II) off Cabo Nazca, taken on 3 and 4 April. Section I was made about 55 km to the southeast of the current meters, which registered poleward flow at the time; Section II was made at the array site when the measured currents were equatorward.

The geostrophic sections are shown in Figures 7a and 7b. The speeds at the offshore deep stations are based on the assumption of

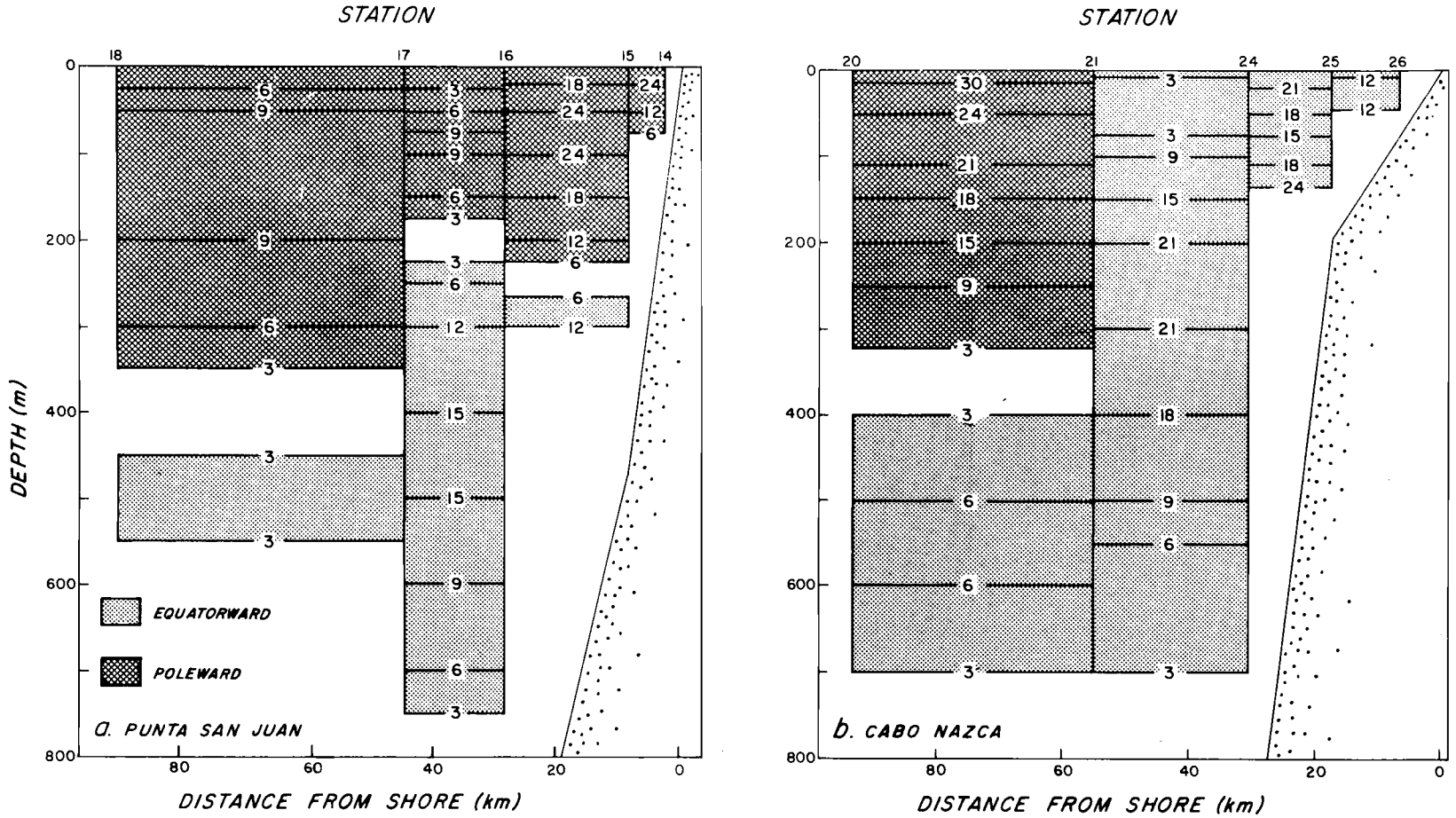

Figure 7. Vertical distributions of geostrophic speeds (cm/sec).

negligible motion at 800 m depth. The speeds over the continental shelf (nearshore) are also geostrophic computations, but are adjusted to the mean observed currents at 50 m during the times the shallow stations were taken.

Wyrtki (1963) has discussed the use of 1000 m as a reference surface off the coast of Peru. Although it was not convenient to use 1000 m as a reference for this study, the motion at 800 m is not significantly different from that at 1000 m when contrasted to the speeds near the surface. The use of current meter references at 50 m, over the shelf, was prompted by three considerations:

(i) the 50 m flow was relatively unaffected by the surface and bottom boundaries;

(ii) both instrument moorings had current meters at 50 m;

(iii) hydrographic samples were taken at 50 m.

Two hypotheses are implicit in the construction of these sections: (a) that the true flow was geostrophic, and (b) that the flow was essentially uniform (synoptically) along the coast.

The difficulties involved in assuming geostrophy over a continental shelf have been discussed by Reid, Roden and Wyllie (1958). In spite of these problems, the geostrophic assumption is consistent with the fact that the geostrophic shears over the shelf were not significantly different from the observed current shears, i.e., in both cases the current field was fairly uniform.

The second hypothesis is equivalent to assuming that an offshore profile taken anywhere along the coast at a given time would yield a similar field of current. The assumption is made as an expedient in order to assign a current meter reference for the first section, which was taken to the southeast of the instrument array. Though the assumption is somewhat arbitrary, it is the most straightforward hypothesis consistent with the data.

The geostrophic speeds in the first section (Figure 7a) were poleward throughout most of the upper 200 to 300 m. At distances of 30 km or more offshore, the maximum (poleward) speeds were about 9 cm/sec, and were centered at depths near 100 m. This flow is consistent with descriptions of the Peru-Chile Undercurrent given by Wooster and Gilmartin (1961) and Wyrtki (1963). The presence of poleward flow near the surface is consistent with Wyrtki's (1966) statement that north of 15° S. the undercurrent is found immediately below a shallow layer of equatorward wind drift. Nearshore the geostrophic speeds were also poleward but of greater magnitude, with a maximum of 24 cm/sec centered at depths near 75 m. This feature suggests that the poleward flow registered over the shelf by the current meters constituted a shoreward extension (and intensification) of the Peru-Chile Undercurrent.

In the second section (Figure 7b) the poleward flow was limited to distances of more than 60 km offshore, occupying the upper 300 m,

and was considerably more intense than the offshore flow of the first section.

The geostrophic flow between stations 21 and 24 (Figure 7b) was equatorward, as was the adjacent flow over the shelf, at the current meters. The similarity of the adjacent flows, based upon independent references (i.e., no motion at 800 m versus observed currents at 50 m), supports the assumption of geostrophy discussed earlier.

The magnitudes of the poleward speeds offshore in Figure 7b were similar to those of the poleward flow over the shelf in Figure 7a. This suggests that the poleward flow observed over the shelf moved offshore during the three day lapse between sections. This is consistent with the fact, already noted in the discussion of Figure 6, that the equatorward flow appeared first at the inshore current meters, seeming to displace the poleward current seaward.

The total poleward transports for Figures 7a and 7b were computed in order to compare them with previous estimates by others for the Peru-Chile Undercurrent. A transport of 2.3 million cubic meters per second was computed for Figure 7a, and 2.0×10^6 m^3/sec for Figure 7b. Wyrtki (1963) estimated a transport of 0.5 to 1.0×10^6 m^3/sec using geostrophic data which did not extend over the shelf.

The descriptions given above may be summarized as follows:

(1) The first section (Figure 7a) exhibited geostrophic flow in the upper 200 to 300 m, at distances of 30 to 100 km offshore. The dimensions, intensity and transport of this flow were similar to those of the Peru-Chile Undercurrent, as described in the literature.

(2) Certain similarities between the geostrophic and observed flows suggest that the poleward flow observed over the shelf was quasi-geostrophic and constituted a shoreward extension (and intensification) of the Peru-Chile Undercurrent.

(3) During the three days between sections the poleward flow observed over the shelf seemed to be displaced seaward as equatorward current appeared nearshore.

The simplest explanation (consistent with the above descriptions) that can be suggested for the observed current behavior is that the poleward flow, probably the Peru-Chile Undercurrent, moved further offshore. It should be noted, however, that the data coverage is not adequate to specify a unique mechanism. For example, the assumption of synoptic uniformity along the coast is not independently verifiable, due to the lack of current meter data at both hydrographic lines. If this assumption is not made, it is possible to show that the observed currents are not inconsistent with the flow predicted by Buchwald and Adams (1968) for a continental shelf wave

propagating in the poleward direction.

Drogue Analysis

The drogues and pertinent wind data have been listed in the order of launch, in Table 3. Due to the pursuit of other scientific activities the drogues could not be tracked between launch and recovery. Radar fixes at launch and recovery, based on points of land, yielded a net displacement for each drogue. An intermediate fix for drogue three resulted in two separate displacements, '3a' and '3b'. Single wind readings were taken from the ship's aerovane at each launch, and are included in Table 3. The mean wind direction and speed for each drogue displacement were computed from the recorded winds at the offshore mooring. The mean values will be referred to in the succeeding discussion, since they were considered more representative of average conditions.

Each drogue was set for a prescribed depth by suspending a current cross from a surface float. The current cross of the first drogue was set at 3.5 meters, and the succeeding six were set for ten meters. An implicit assumption, which depends upon the response of the drogue and the quality of the navigational fixes for its validity, is that the observed displacements are representative of motion at the depths for which the drogues were set. An error discussion pertinent to these considerations is presented by Knauss

Table 3. Drogue statistics.

Drogue	Date	Depth (m)	Total time (hours)	Drogue		Ship's wind		Average wind	
				speed (cm/sec)	direction (degrees)	speed (knots	direction (degrees)	speed (knots)	direction (degrees)
1	3-30	3.5	4.0	21	050	17	170	11.0	169
2	4-5	10	2.5	19	337	6	190	6.8	173
3a	4-5	10	2.0	26	360	10	180	9.9	167
3b	4-5	10	3.5	16	180	10	180	8.3	158
4	4-6	10	5.0	19	350	12	160	9.0	163
5	4-7	10	5.7	5	205	5	140	7.4	156
6	4-8	10	8.0	9	335	12	170	9.5	159
7	4-8/9	10	28.0	17	168	5	150	5.6	166

(1963). The drogues set during the PISCO study were of short duration, thereby amplifying the effects of navigational errors on the velocity determinations. The radar fixes themselves were relatively accurate, however, since they were based upon land references.

The locations and times of the drogues may be visualized in relation to the moored instrument data by referring to Figures 1, 3, and 6. All but the fifth drogue were set within 20 km of the instrument array (Figure 1). Drogues two and three were set toward the end of the equatorward 'event' at the current meters (Figures 3, 6); drogues four through seven were set during poleward flow at the current meters.

It can be seen from Table 3 that the ten meter drogue displacements, with the exception of drogue two, were toward the north for winds of nine knots or more. Other displacements at ten meters were to the south. Notice also that the displacements for drogues six and seven overlapped in time. Drogue six moved to the north for a mean wind speed of 9.5 knots, while drogue seven moved to the south for a mean wind speed of 5.6 knots. Drogue two moved toward the northwest for a mean wind of 6.8 knots, thereby not conforming to this pattern.

Figure 8a consists of a series of vector roses for the various drogue settings at ten meters. Each vector rose includes: (i) the velocity vector for the drogue displacement, $\overline{D}$; (ii) the average current vector at 25 m inshore, $\overline{A}$; (iii) the average current vector at

25 m offshore, $\overline{C}$; (iv) the average wind vector, $\overline{W}$. All current and wind averages were computed from the moored instrument data for the periods of the drogue displacements. The symbols $\overline{A}$ and $\overline{C}$ were chosen for easy reference to the daily mean currents shown in Figure 6.

Figure 8a shows that drogue two was the only one for which the 25 m currents were predominantly northwestward, thus explaining its somewhat anomalous behavior as seen in Table 3. The remaining vector roses illustrate graphically how the drogues tended to move with the southeastward flow at 25 m, except for winds of nine knots or more.

The drogue behavior confirms what one would qualitatively expect for a wind drift layer overlying a field of flow which is opposite to the wind. The ten meter motion reflected the influence of both the wind and the 25 m flow. It can be seen from Figure 6 that the 25 m currents were quite similar to those at 50 m, but showed no noticeable dependence on the wind. It may be concluded then that the depth of the wind drift layer was between 10 m and 25 m.

Figure 8b presents vector roses for drogues four through seven, when the 25 m flow was similar (southeastward) at both moorings. The two 25 m current vectors are replaced by their average, $\overline{V} = \frac{1}{2}(\overline{A} + \overline{C})$, and the vector difference, $\overline{D} - \overline{V}$, is also shown. The vector $(\overline{D} - \overline{V})$ represents the drogue displacement relative to the

Figure 8. Vector roses for 10 m drogues, observed currents at 25 m, and observed winds.

D = Drogue velocity vector at 10 m.

W = Wind velocity vector.

A = Current velocity vector at 25 m, inshore.

C = Current velocity vector at 25 m, offshore.

V = 1/2 (A + C)

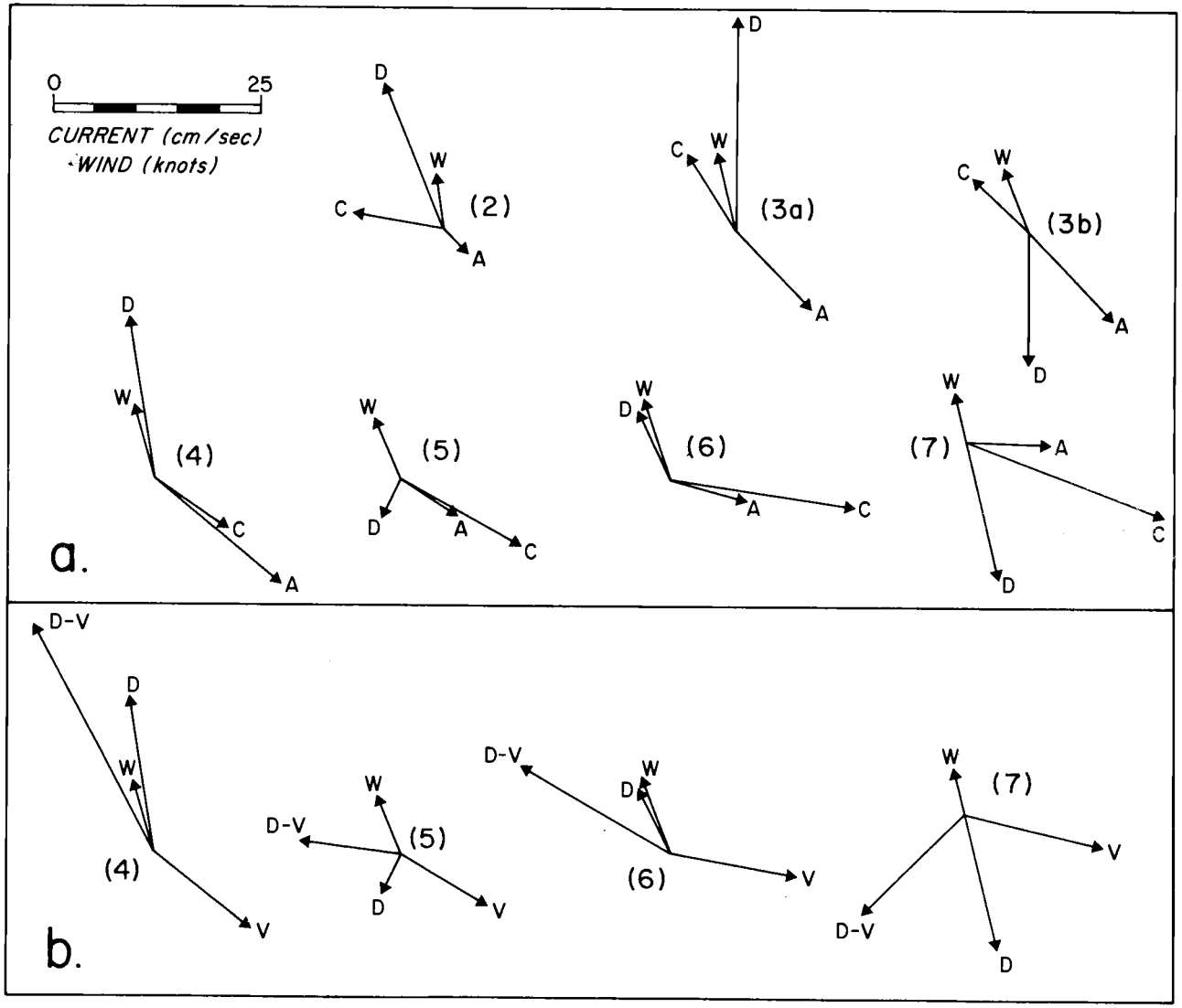
0
25
CURRENT (cm/sec)
WIND (knots)
(2)
(3a)
(3b)
(4)
(5)
(6)
(7)
a.
b.
D
W
C
A
D-V
V

estimated flow at 25 m, $\overline{V}$, and therefore is an estimate of the drogue displacement, had there been no net current at 25 m. In all cases $(\overline{D}-\overline{V})$ was directed to the left of the wind vector, $\overline{W}$, in the sense expected from the Ekman model. This exercise cannot be meaningfully performed for drogues two and three, since the 25 m flow was not uniform in those instances.

The results of the drogue analysis may be summarized as follows:

(1) when the 25 m flow was predominantly northwestward, drogue displacements were northward, in accordance with the wind;

(2) when the 25 m flow was uniformly southeastward, drogue displacements were southward for winds of less than nine knots, and northward otherwise;

(3) the data suggest that the wind drift layer was between 10 m and 25 m thick;

(4) when the 25 m flow was uniformly southeastward, drogue displacements were in the sense expected from the Ekman model.

VI. UPWELLING CONDITIONS

Two sources of data are used for the description of upwelling conditions during the PISCO study:

(i) vertical sections of density anomaly (sigma-t), dissolved oxygen, and nitrate, corresponding to the hydrographic lines shown in Figure 1;

(ii) horizontal surface maps of temperature, nitrate, and chlorophyll 'a' constructed from the underway surveys over the continental shelf.

Because of the similarity between the distributions of temperature and sigma-t, vertical temperature sections are not presented. Discussions of salinity are deferred to the last chapter.

The locations and times of the hydrographic distributions will be identified in the discussion, however, the reader may refer to Figures 1 and 3 for additional spatial and temporal orientation.

Figure 9a is the vertical section of density anomaly (sigma-t) off Punta San Juan on 31 March and 1 April (Section I). The depth scale of the upper 100 m has been expanded for added clarity. The current meters over the continental shelf registered poleward flow at this time. A pycnocline extended from 10 m to 70 m, with the greatest density gradient at 15 m, offshore. At depths of less than 70 to 80 m the isograms of density rose toward the coast, forming

an inclined frontal layer. At depths of more than 80 m the isograms sank in the shoreward direction.

Figure 9b is the vertical section of sigma-t off Cabo Nazca on 3 and 4 April. The current meters over the shelf registered equatorward flow at this time. The pycnocline offshore extended from 10 m to 60 m and was most intense at 15 m. A well defined frontal layer was not formed as in Figure 9a, due to the shoreward spreading of the isograms. At the offshore stations the shoreward rise of isograms was limited to the upper 30 m; nearshore the isograms rose from depths of 80 m or less.

Both sections in Figure 9 show evidence of upwelling over the continental shelf; the depth of the upwelling, based upon the shoreward rise of isograms was about 75 m. This is in agreement with Wyrtki (1963), who estimated that upwelling off Peru was limited to the upper 100 m. Below 100 m the density surfaces tended to sink shoreward, resulting in a weak density gradient between 75 m and 100 m. This feature is often (but not invariably) associated with coastal undercurrents. Mooers (1969) has given an excellent account, in terms of the thermal wind effect, of how this relationship occurs. Yoshida and Tsuchiya (1957) stipulate that such a shoreward spreading of density surfaces may be considered an indicator of upwelling.

Caution must be exercised in the interpretation of Figures 9a and 9b, since the hydrographic lines were separated in both time and

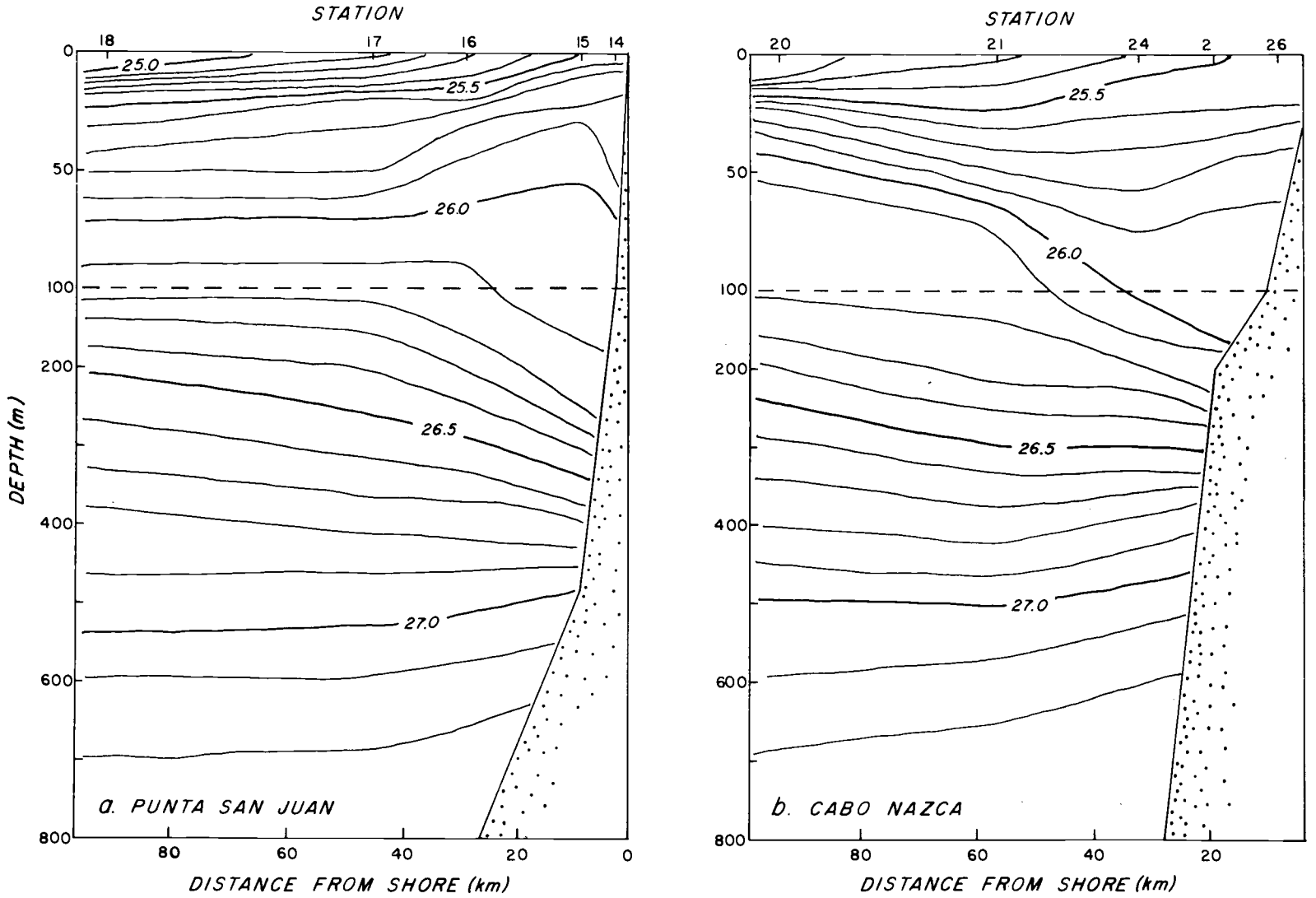

Figure 9. Vertical distributions of density anomaly (sigma-t).

space. Thus it cannot be stated without further evidence that the subsidence of density surfaces offshore in Figure 9b was related to a breakdown of the frontal layer during upwelling. Alternative hypotheses are that the observed differences were related to temporal and spatial changes in the coastal circulation, or that independent pockets of upwelling activity were observed, and so forth.

Figure 10 illustrates the vertical distributions of dissolved oxygen (milliliters per liter) and nitrate (microgram-atoms per liter) for the section off Punta San Juan (31 March). Near the surface and close to shore, newly upwelled water is indicated by high nitrate (18 μg-at/l) and low oxygen saturation (60%). In contrast, the nitrate concentrations offshore were low (6 μg-at/l) and oxygen was supersaturated (113%), reflecting previous, or already established phytoplankton activity. Similar features can be seen in the vertical distributions off Cabo Nazca, on 3, 4 April (Figure 11).

During the survey phase of the cruise, the Data Acquisition System analyzed temperature, nitrate, silicate, and chlorophyll 'a' at 3 m while the ship was underway, and 'surface' maps of these properties were plotted. The operational aspects of the surveys are discussed in Chapter three in greater detail.

For this thesis, some of the original maps from short, consecutive surveys were combined to produce sets of longer maps for analysis. Four sets of maps are presented in Figure 12, each set

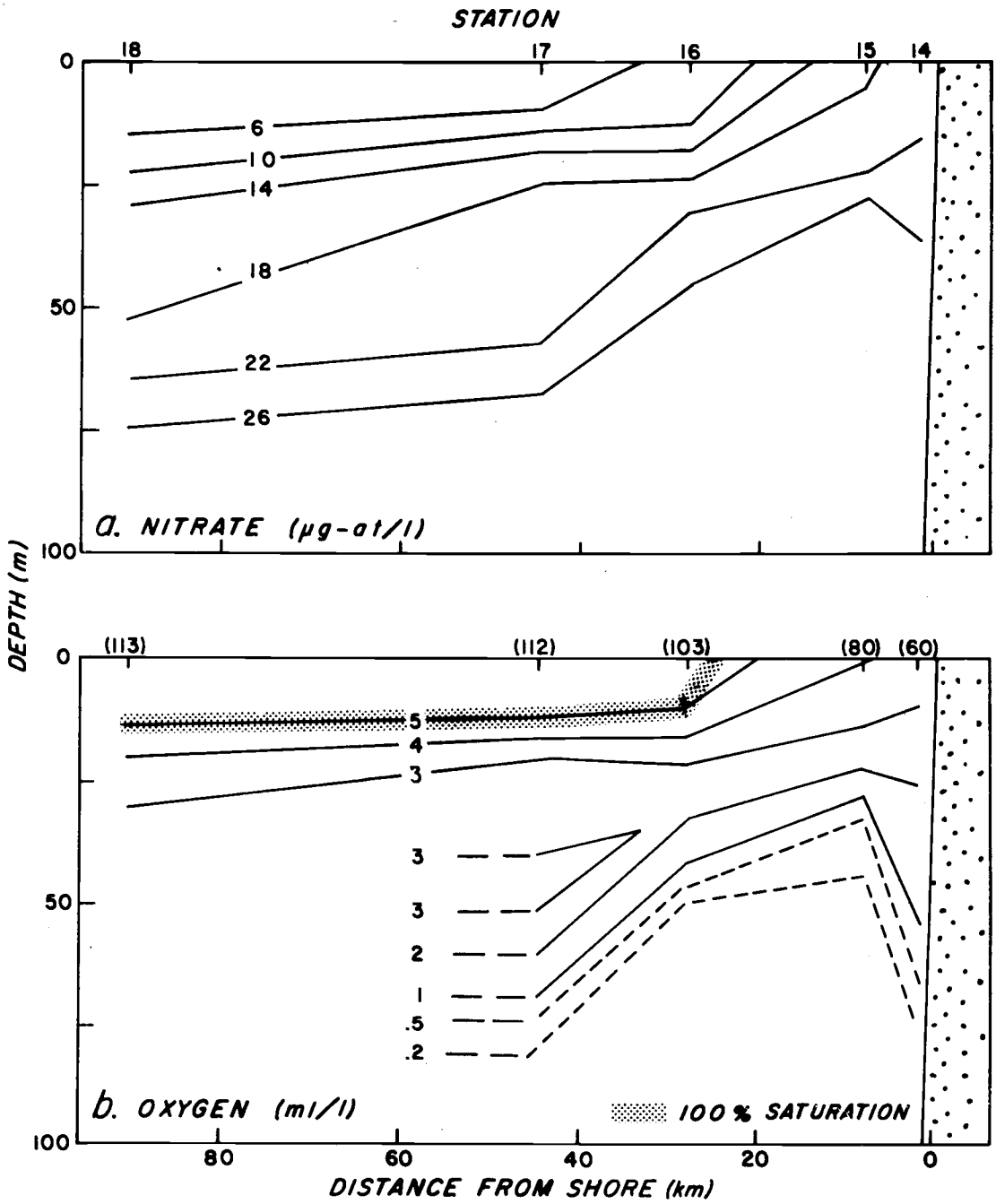

Figure 10. Vertical distributions of nitrate and dissolved oxygen off Punta San Juan. (31 March and 1 April). Numbers in parentheses indicate oxygen saturation values at the surface.

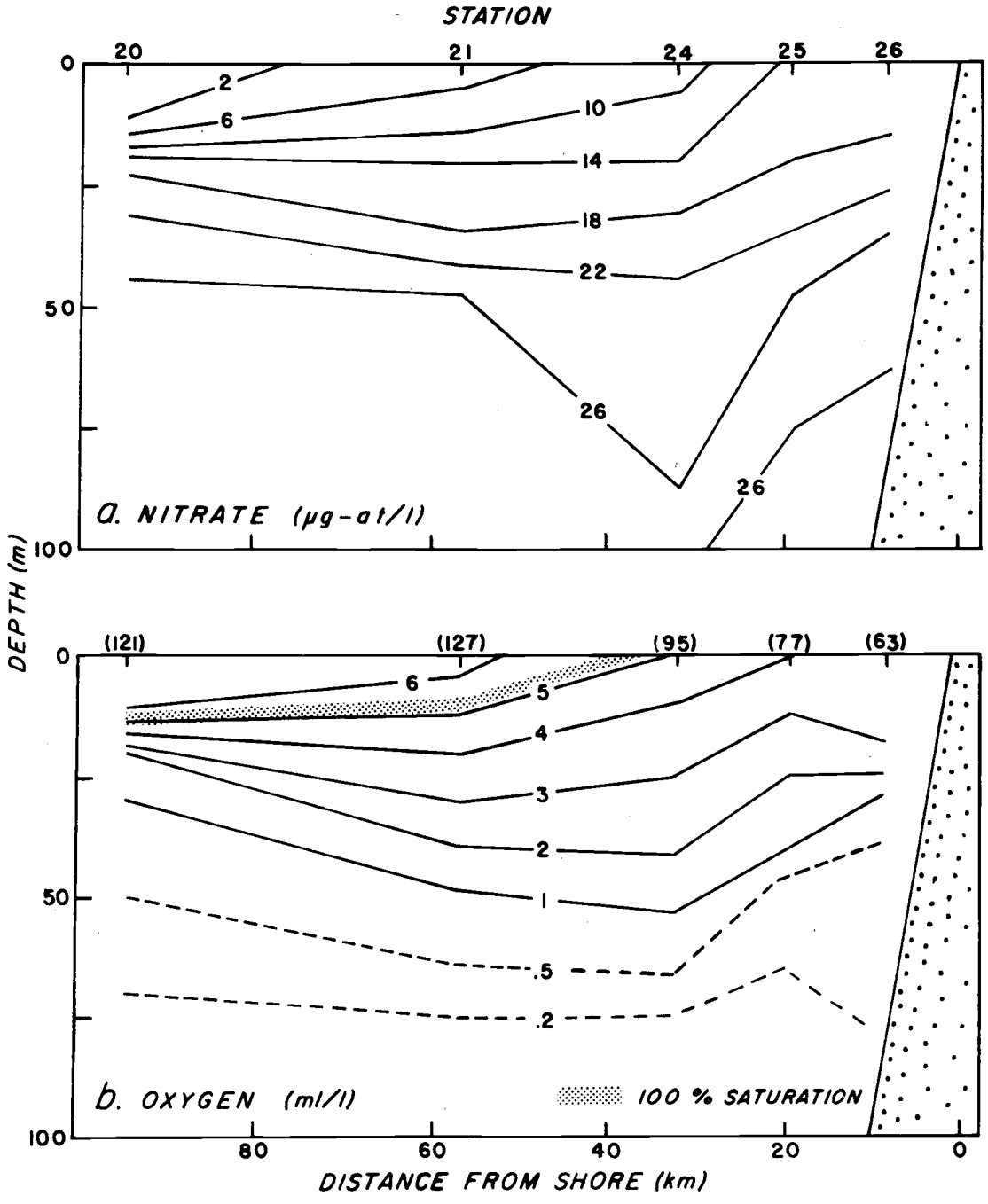

Figure 11. Vertical distributions of nitrate and dissolved oxygen off Cabo Nazca (3 and 4 April). Numbers in parentheses indicate oxygen saturation values at the surface.

Figure 12. Maps of the surface distributions of temperature, nitrate, and chlorophyll 'a'.

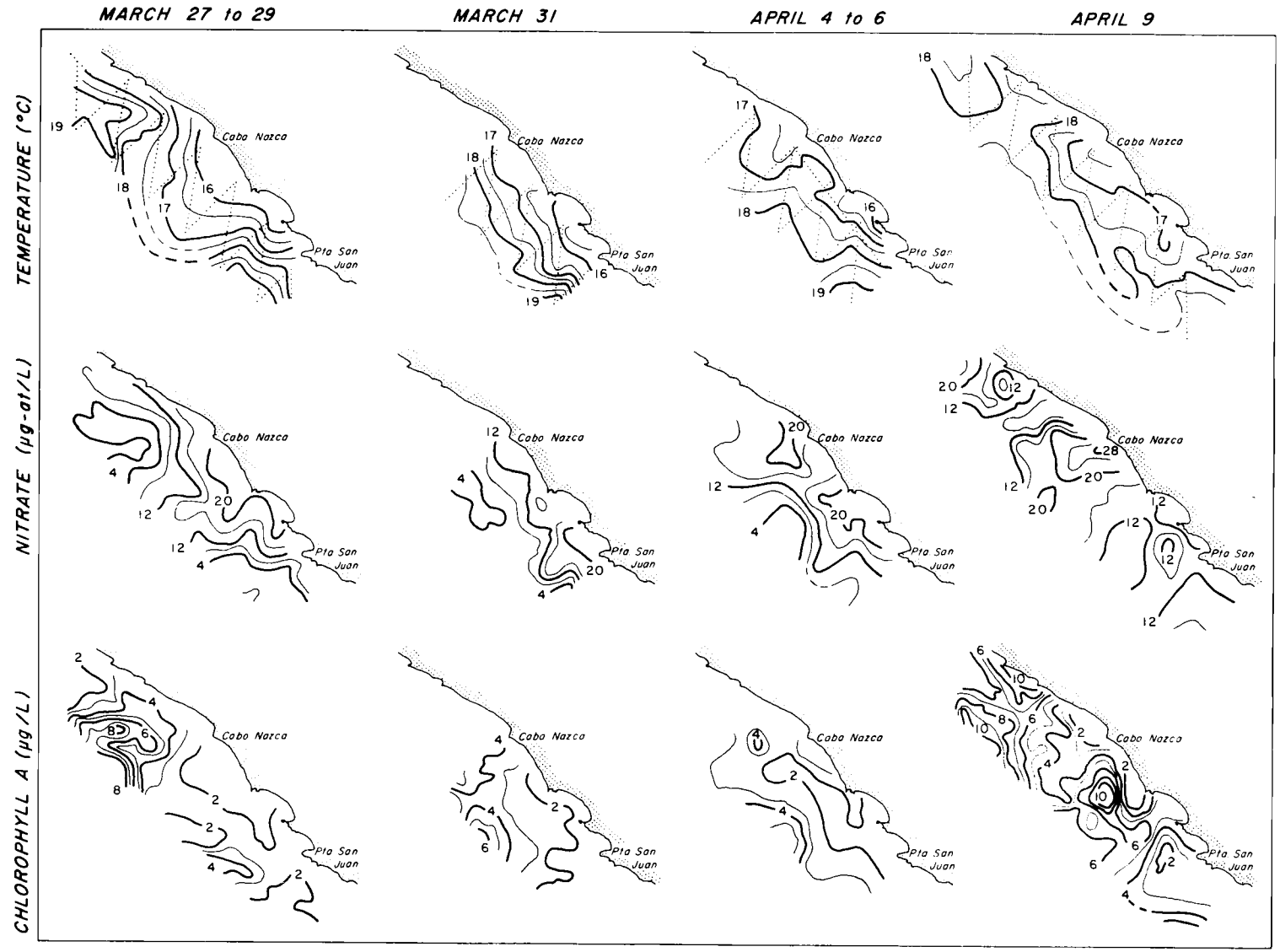
MARCH 27 to 29
MARCH 31
APRIL 4 to 6
APRIL 9
TEMPERATURE (°C)
NITRATE (µg-at/L)
CHLOROPHYLL A (µg/L)
Cabo Nazca
Pta San Juan

containing separate maps for temperature, nitrate, and chlorphyll 'a'. The survey track for each set is shown by a dotted line on the corresponding temperature distribution. The maps may be spatially and temporally visualized with respect to other data by referring to Figures 1 and 3.

The synopticity of such maps depends upon the effects of advective and biological changes during the surveys. Several surveys run on consecutive occasions overlapped each other partially, and the major features of the contours could still be recognized from one survey to the next. This was most evident for temperature distributions, but was also observed for nitrate. Chlorophyll 'a' had the poorest synoptic characteristics due to the relatively rapid, non-conservative changes which it undergoes. For example, the first set of maps (March 27 to 29) is the product of two separate surveys which were 'spliced' near Cabo Nazca. The noticeable differences in chlorophyll to either side of this juncture were probably not synoptic, but instead reflect changes occurring between surveys. For this discussion it will be assumed that the maps were quasi-synoptic over periods of two days or less, with some reservations in regard to Chlorophyll 'a'.

Centers of recently upwelled water are manifested by nearshore 'pockets' of low temperature and high nitrate. Because of non-conservative changes in chlorophyll 'a', this constituent is not a good

indicator of upwelling centers. But values near the coast remained low throughout the period, in spite of large changes elsewhere. Thus, phytoplankton populations were probably low close to shore, which is consistent with newly upwelled water. At all times, a center of freshly upwelled water was found between Cabo Nazca and Punta San Juan. The intensity of upwelling activity appeared to be modulated in space and time. For example, on 31 March the upwelling appeared more intense at Punta San Juan than at Cabo Nazca; on 9 April the reverse was the case.

VII. CURRENTS IN RELATION TO UPWELLING

It has been seen from current meter observations (Figures 4, 6) that the flow over the continental shelf was poleward during most of the observation period. Comparison with geostrophic speeds suggests that this flow may have been a shoreward extension of the Peru-Chile Undercurrent. Neither the geostrophic nor observed shears were large over the shelf, the flow being essentially quasi-barotropic. Three days of equatorward flow occurred at the current meters, during which the previous poleward flow appeared to have moved offshore.

Hydrographic data (Figures 9-12) revealed evidence for upwelling activity between Cabo Nazca and Punta San Juan throughout the study period. Centers of relatively intense upwelling could be distinguished close to shore (Figure 9) where temperatures were low and nitrates were high. The intensity of upwelling activity was modulated in space and time, as seen from the distribution of upwelling centers.

Both upwelling and currents are known to interact with the field of mass in coastal areas where upwelling occurs. A causal relationship may therefore exist between the respective changes observed in the currents and upwelling. A factor to be considered in any such relationship is the wind, which is known to induce upwelling.

In order to see if an apparent correlation existed, the approximate sequences of observed currents, upwelling, and wind are presented in Table 4. Four phases are distinguished, corresponding to the four upwelling situations shown in Figure 12. The sequences of currents and wind can be seen graphically in Figure 6. The ratio of nitrate to temperature at Cabo Nazca (the current meter site) is presented as a measure of upwelling intensity there.

It can be seen from Table 4 that the currents, upwelling and wind are modulated in some cyclic fashion, however it is difficult to discern any meaningful relationships between them. This is not surprising, since the changes took place on a time scale of about a week, or half the observation period, and were observed only in the vicinity of Cabo Nazca. Thus, the areal coverage and duration of the data are not sufficient to adequately define the processes and their correlations, if such exist.

The currents might not only be related to upwelling through dynamic interactions. For example, the water which supplies the upwelling at some depth is presumably imported into the upwelling area by a current or combination of currents. It was shown in Chapter 6 that the upwelling during the PISCO study was limited to depths of some 75 m or less, in agreement with Wyrtki (1963). It can be asked what kind of water was found in, say, the upper 100 m offshore, and how it got there.

Table 4. Comparison of changes in currents, upwelling, and wind.

Dates	Observed currents	Nitrate (μg-at/l) / Temperature (°C)	Wind (knots)
27 March to 29 March	poleward	20/16.0 = 1.3	10
31 March	poleward	12/17.0 = 0.7	8
4 April to 6 April	equatorward	20/16.5 = 1.7	10 to 5*
9 April	poleward	28/16.5 = 1.7	5

*Speeds decreasing from 10 knots to 5 knots

The vertical salinity distributions for the two hydrographic lines shown in Figure 1 are presented in Figure 13. Figure 13a is the salinity section off Punta San Juan on 31 March and 1 April. In general, salinity decreased with depth from 35.06‰ at the surface to 34.55‰ below 500 m. In addition, a weak minimum was present above 100 m at stations 16, 17, and 18, being most noticeable at a depth of 75 m at station 17. The general features of Figure 13b (Cabo Nazca, 3 and 4 April) are similar, however the salinity minimum is seen only at station 20, furthest offshore.

The water masses normally found in the coastal area near 15° S. were discussed in the LITERATURE REVIEW. Subtropical Surface Water, Equatorial Subsurface Water (or Equatorial Pacific Water according to Sverdrup et al., 1942) and Subantarctic Water are observable in the upper 200 m.

Temperature-salinity curves for station 17 of the PISCO cruise, and station 8 of the STEP-I expedition (Wyrtki, 1963) are shown in Figure 14. Station 8, taken during the spring (southern hemisphere) of 1960, was located several hundred kilometers off Punta Aguja, Peru, near 7° S. In his discussion of station 8, Wyrtki pointed out that the temperature-salinity regression below 100 m was Equatorial Subsurface Water, and the almost isohaline water above 100 m he characterized as Equatorial Subsurface Water upwelled near the coast and subsequently transported seaward. The curves for stations 8 and 17 compare well with each other, except for the weak salinity

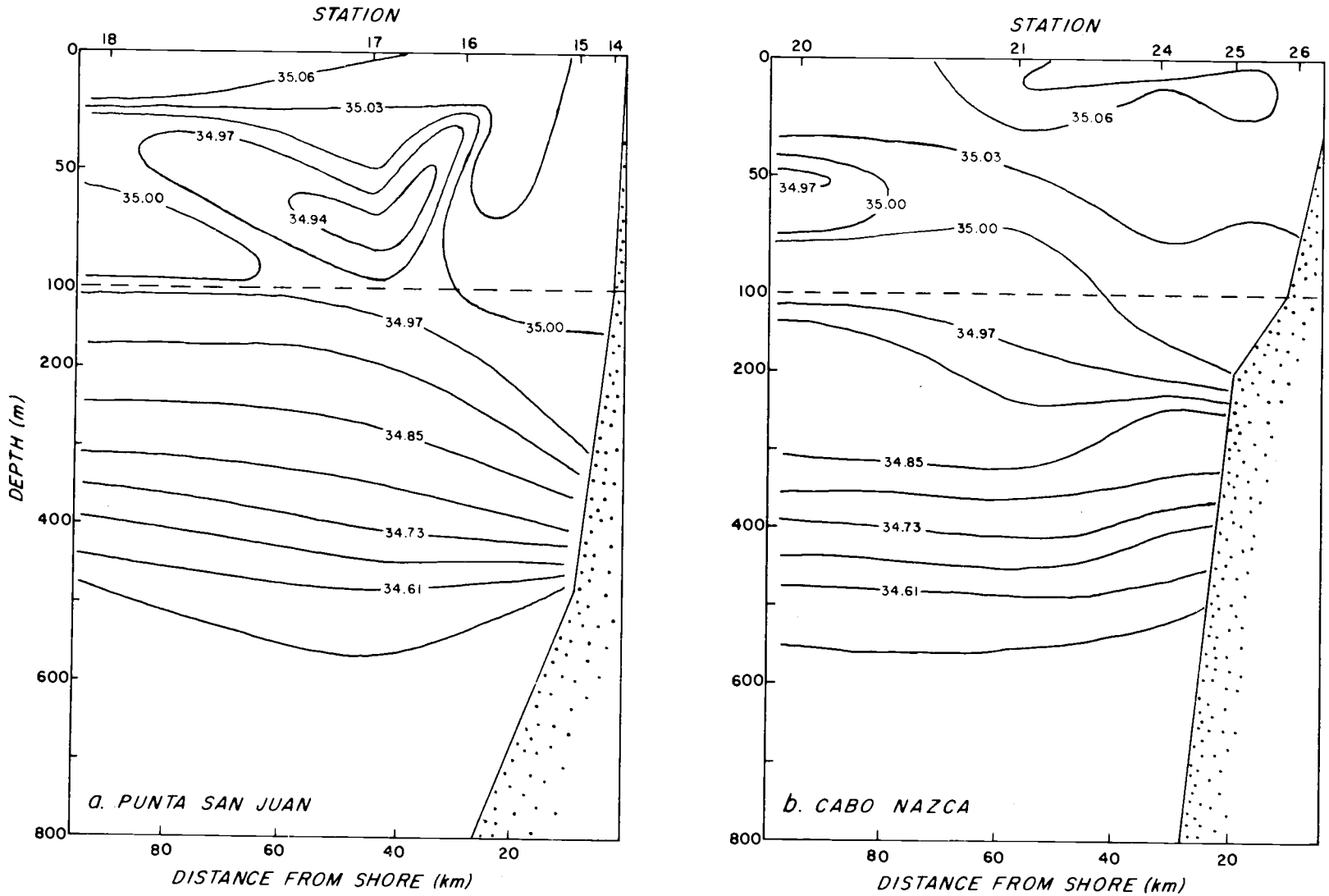

Figure 13. Vertical distributions of salinity (‰).

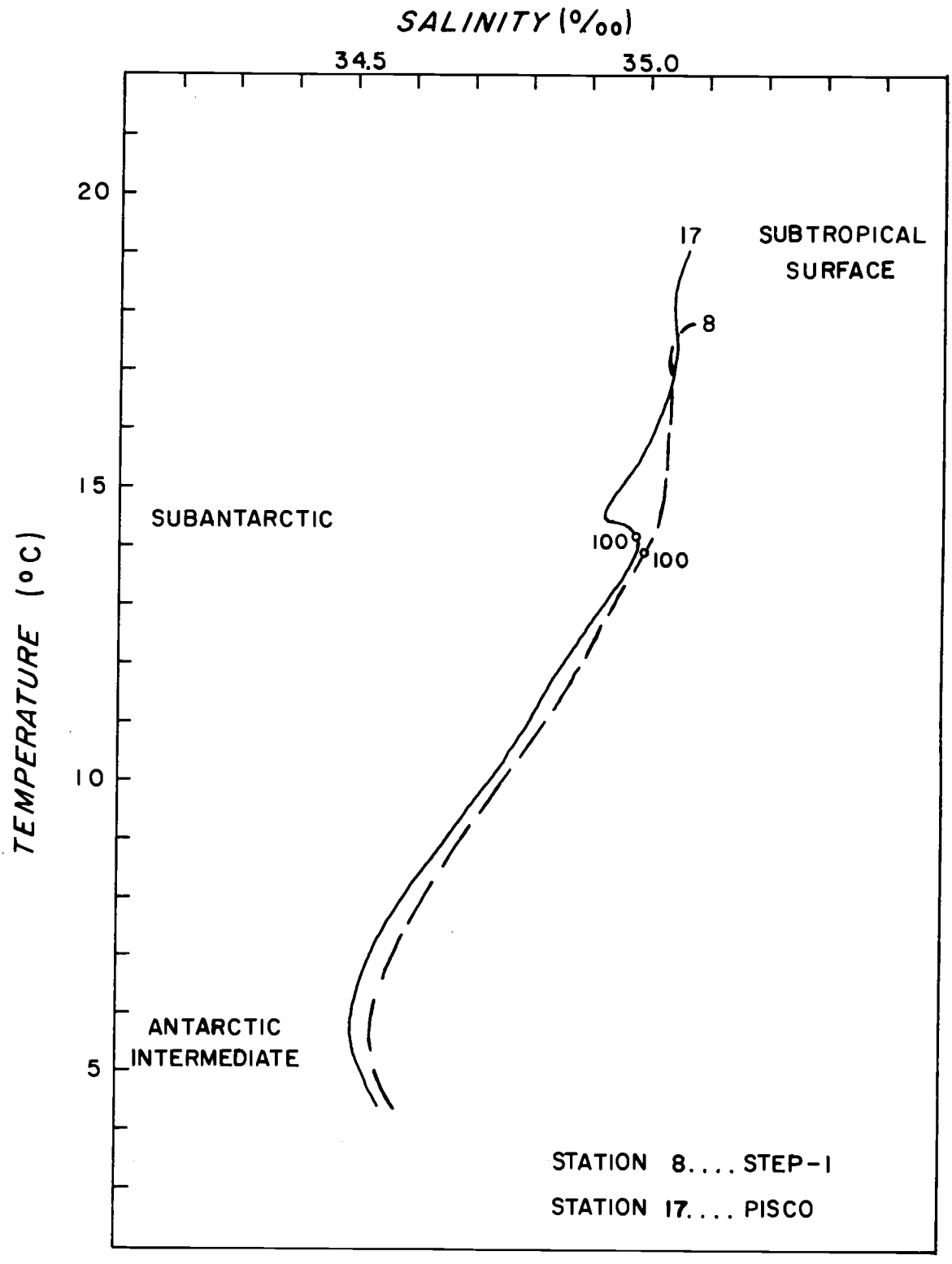

Figure 14. Temperature salinity curves for Station 8 (STEP-I expedition) and Station 17 (PISCO cruise). Small open circles indicate 100 m depth.

minimum at station 17.

There is no precipitation or runoff of any consequence along most of the Peruvian coast. The only source of relatively fresh water is therefore the Subantarctic Water, which presses equatorward from higher latitudes as far as about 15° S. The salinity minimum of station 17 is apparently a remnant of Subantarctic Water embedded in a much larger mass of Equatorial Subsurface Water.

It is to be noted that the salinity minimum was not present at all stations during the Pisco study, as seen from the salinity sections of Figure 13. In particular, it was not present over the continental shelf, which is evidence of the active upwelling and mixing which took place there.

Comparison of Figure 13 with the geostrophic speeds in Figure 7 reveals that the salinity minimum was only found in conjunction with poleward flow. This is curious, because one would naively expect the opposite, namely, that low salinity water would be introduced from the south. A possible explanation is that low salinity water was carried equatorward originally, by the Peru Coastal Current, but further offshore than the limits of this study. Somewhere north of the hydrographic sections, this water may have been brought coastward, either by advection or lateral mixing, into the range of the Peru-Chile Undercurrent. After returning to the southeast, the undercurrent and salinity minimum appeared to be displaced offshore by the

equatorward flow which was observed to originate in the well mixed water over the shelf (and which therefore contained no salinity minimum).

To the casual reader, this explanation might appear forced. But there is considerable evidence, from geopotential topographies and maps of acceleration potential (Wyrtki, 1963; White, 1969), that the Peru Coastal Current does in fact move coastward to the north of 15^{o} S. It may be that large quantities of water reach the upwelling areas south of 15^{o} S. by means of this circuitous route.

VIII. SUMMARY AND CONCLUSIONS

Hydrographic observations and data from moored instruments were used to describe the coastal currents and upwelling conditions off Peru.

The field of observed currents was quasi-barotropic during most of the period, that is, the currents behaved in a similar manner at different locations over the continental shelf. The observed flow was poleward except for a three day interruption, or 'event', of equatorward flow. A comparison of the observed currents with geostrophic sections indicates that the poleward flow over the shelf may have been a shoreward extension of the Peru-Chile Undercurrent. The data also suggest that this current moved further offshore as the equatorward flow was observed over the shelf. Geostrophic transports for the poleward flow, both offshore and over the shelf, were estimated at about 2×10^6 m^3/sec.

Autospectra computed for the time series of current revealed significant semidiurnal energy in the longshore component of flow. The estimated amplitudes of the tidal oscillations were about ten to 15 percent of the period mean speeds. The results were consistent with a small amplitude, progressive, semidiurnal tide propagating along the coast.

Winds during the period were consistently from the southeast and showed a general decreasing trend in speeds. A prominent

sea-breeze oscillation was observed during the entire study.

Ten-meter drogue displacements reflected the influence of the observed winds and of the observed flow at 25 m. During a period of quasi-barotropic poleward flow over the shelf, the drogues were observed to move with the 25 m flow and against the wind, except when wind speeds were about nine knots or greater. Drogue displacements were in the sense expected from the Ekman model. The depth of the wind drift layer was estimated at 10 m to 25 m.

Distributions of properties, based upon hydrographic casts and underway surface surveys, indicated upwelling activity between Cabo Nazca and Punta San Juan throughout the study period. Centers of relatively intense upwelling were indicated close to shore, where temperatures were low and nitrates were high. The intensity of upwelling activity appeared to be modulated in space and time, as seen from the distribution of upwelling centers.

Sequences of changes in currents, upwelling, and winds were compared to see if causal relationships between them could be discerned. It was concluded that the areal coverage and duration of the data was not adequate to make such determinations, due to the relatively large time and space scales involved.

The principal water mass in the upwelling area was found to be Equatorial Subsurface Water. A weak salinity minimum was found at some stations, offshore, at depths of 30 to 75 meters. It is

concluded that this minimum represents the remnants of Subantarctic Water, which is known to reach as far north as 15° S. The occurrence of this minimum only with poleward flow suggests that it was first carried north of 15° at greater distances off the coast. At some distance to the north of the study area, it may have been subsequently entrained coastward into the Peru-Chile Undercurrent and returned southward.

BIBLIOGRAPHY

Armstrong, F. A. J., C. R. Stearns and J. D. H. Strickland. 1967. Measurements of upwelling and subsequent biological processes by means of the Technicon Autoanalyzer and associated equipment. Deep Sea Research 14:381-389.

Bogdanov, K. T. 1961. New charts of the cotidal lines of the semi-diurnal tidal waves (M_2 and S_2) for the Pacific Ocean. Oceanology 136-141:28-31. (Translated from Doklady Academia nauk SSSR)

Buchwald, V. T. and J. K. Adams. 1968. The propagation of continental shelf waves. Proceedings of the Royal Society, ser. A, 305:235-250.

Collins, C. A. 1968. Description of measurements of current velocity and temperature over the Oregon continental shelf, July 1965 - February 1966. Ph. D. thesis. Corvallis, Oregon State University. 153 numb. leaves.

Guillén, O. and L. A. Flores. 1967. Informe preliminar del crucero 6702 del verano de 1967 (Cabo Blanco - Arica). Boletín del Instituto del Mar del Perú - Callao 18:1-17.

Gunther, E. R. 1936. A report on oceanographical investigations in the Peru Coastal Current. Discovery Reports 13:107-276.

Hart, T. J. and R. I. Currie. 1960. The Benguela Current. Discovery Reports 13:123-298.

Knauss, J. A. 1963. Drogues and neutral-buoyant floats. In: The sea, ed. by M. N. Hill. Vol. 2. New York, Interscience. p. 281-282.

Mejía, J. and L. A. Poma. 1966. Informe preliminar del crucero de otoño de 1966 (Cabo Blanco -Ilo). Boletín del Instituto del Mar del Perú - Callao 13:1-31.

Miñano, J. 1968. Informe preliminar del crucero 6705-06 del otoño de 1967 (Cabo Blanco - Ilo). Boletín del Instituto del Mar del Perú 21:1-13.

Mooers, C. N. K. 1969. The interaction of an internal tide with the frontal zone in a coastal upwelling region. Ph. D. thesis. Corvallis, Oregon State University. 480 numb. leaves.

Mooers, C. N. K., Lillie M. Bogert, Robert L. Smith and June G. Pattullo. 1968. A compilation of observations from moored current meters and thermographs (and of complementary oceanographic and atmospheric data). Corvallis. 98 numb. leaves. (Oregon State University. Dept. of Oceanography. Data report no. 30 on National Science Foundation Grant GA 331, Reference 68-5, June 1968)

Pillsbury, R. D., R. L. Smith and R. C. Tipper. 1969. A reliable low cost mooring system for oceanographic instrumentation. Limnology and Oceanography 14:307-311.

Posner, G. S. 1957. The Peru Current. Bulletin of the Bingham Oceanographic Collection, Yale University 16(2):106-155.

Reid, J. L., G. I. Roden and J. G. Wyllie. 1958. Studies of the California Current system. In: Progress report of the California Cooperative Oceanic Fisheries Investigations, July 1, 1956 to January 1, 1958. (Berkeley) California Dept. of Fish and Game, Marine Research Committee. p. 28-57.

Roden, G. I. 1962. Oceanographic aspects of the eastern equatorial Pacific. Geofísica Internacional 2:601-616.

Schweigger, Erwin. 1958. Upwelling along the coast of Peru. The Journal of the Oceanographical Society of Japan 14(3):1-5.

Smith, R. L. 1968. Upwelling. Oceanography and Marine Biology: an Annual Review 6:11-46.

Smith, R. L., C. N. K. Mooers and D. B. Enfield. Mesocale studies of the physical oceanography in two upwelling regions: Oregon and Peru. In: Proceedings of the International Symposium on the Fertility of the Sea, ed. by J. D. Costlow. (In press)

Sverdrup, H. U., M. W. Johnson and R. H. Fleming. 1942. The oceans, their physics, chemistry, and general biology. New York, Prentice-Hall, 1087 p.

White, W. B. 1969. The Equatorial Undercurrent, the South Equatorial Countercurrent, and their extensions in the South Pacific Ocean east of the Galapagos Islands during February-March, 1967. College Station. 74 p. (Texas Agricultural and Mechanical University. Research Foundation. Reference 69-4-T May)

Wooster, W. S. and M. Gilmartin. 1961. The Peru-Chile Undercurrent. Journal of Marine Research 19:97-122.

Wooster, W. S. and J. L. Reid. 1963. Eastern boundary currents. In: The sea, ed. by M. N. Hill. Vol. 2. New York, Interscience. p. 253-280.

Wyrtki, Klaus. 1963. The horizontal and vertical field of motion in the Peru Current. Bulletin of the Scripps Institution of Oceanography 8(4):313-346.

_____ 1966. Oceanography of the Eastern Equatorial Pacific Ocean. Oceanography and Marine Biology: an Annual Review 4:33-68.

Yoshida, Kozo. 1967. Circulation in the eastern tropical oceans with special reference to upwelling and undercurrents. Japanese Journal of Geophysics 4(2):1-75.

Yoshida, Kozo and M. Tsuchiya. 1957. Northward flow in lower layers as an indicator of coastal upwelling. Records of Oceanographic Works in Japan 4(1):14-22.